

Dual RNA-seq unveils noncoding RNA functions in host-pathogen interactions

Alexander J. Westermann¹, Konrad U. Förstner^{1,2}, Fabian Amman^{3,4}, Lars Barquist¹, Yanjie Chao¹, Leon N. Schulte¹, Lydia Müller³, Richard Reinhardt⁵, Peter F. Stadler^{3,4,6,7} & Jörg Vogel^{1,8}

Bacteria express many small RNAs for which the regulatory roles in pathogenesis have remained poorly understood due to a paucity of robust phenotypes in standard virulence assays. Here we use a generic ‘dual RNA-seq’ approach to profile RNA expression simultaneously in pathogen and host during *Salmonella enterica* serovar Typhimurium infection and reveal the molecular impact of bacterial riboregulators. We identify a PhoP-activated small RNA, PinT, which upon bacterial internalization temporally controls the expression of both invasion-associated effectors and virulence genes required for intracellular survival. This riboregulatory activity causes pervasive changes in coding and noncoding transcripts of the host. Interspecies correlation analysis links PinT to host cell JAK-STAT signalling, and we identify infection-specific alterations in multiple long noncoding RNAs. Our study provides a paradigm for a sensitive RNA-based analysis of intracellular bacterial pathogens and their hosts without physical separation, as well as a new discovery route for hidden functions of pathogen genes.

Regulatory RNAs crucially contribute to post-transcriptional control of gene expression in a wide array of organisms, including pathogenic bacteria^{1–3}. The facultative intracellular pathogen *Salmonella enterica* serovar Typhimurium (hereafter referred to as *Salmonella*) expresses hundreds of small regulatory RNAs (sRNAs), many of which are activated under defined stress and virulence conditions^{4–10}, suggesting a role during host infection. Likewise, genetic inactivation of Hfq, a protein required by many sRNAs for target mRNA regulation, attenuates *Salmonella* virulence¹¹. However, deletion of sRNA genes typically results in mild, if any, phenotypes in animal models^{12–14}, probably because most sRNAs act to fine-tune gene expression^{2,3}. Therefore, more sensitive approaches are needed to uncover their molecular functions during infection.

RNA-seq provides a sensitive method for global gene expression analysis in infection biology^{15,16}. However, as bacterial infections of eukaryotic cells involve two interacting organisms with profoundly different transcriptomes, RNA-seq studies are commonly restricted to either the pathogen or host after their physical separation¹⁵. Furthermore, they typically focus on messenger RNAs (mRNAs) as a proxy for protein expression, neglecting the vast RNA output from noncoding regions. Theoretically, RNA-seq should permit a simultaneous profiling of all RNA classes in both intracellular bacteria and the eukaryotic host, despite a striking excess of eukaryotic over bacterial RNA^{15,17}. Such a one-step dual RNA-seq¹⁵ analysis separates transcripts *in silico*, rendering the tedious and error-prone physical separation of pathogen and host superfluous. Here, dual RNA-seq has been used to discover how *Salmonella* sRNAs fine-tune gene expression in intracellular bacteria, with widespread consequences for the human host response.

Dual RNA-seq of *Salmonella*-infected human cells

We established dual RNA-seq for *Salmonella* using HeLa cells in which bacterial invasion is followed by prolonged intracellular replication and a well-defined host response¹⁸ with low TLR activity¹⁹, which helps to

reveal host signalling events directly modulated by the pathogen. We built on previous work²⁰ combining green fluorescent protein (GFP)-expressing *Salmonella* and fluorescence-activated cell sorting (FACS) to select host cells containing on average 10 or 75 bacteria at 4 or 24 h post-infection (p.i.), respectively, and also non-invaded control cells (Fig. 1a and Extended Data Fig. 1a–d). Optimized fixation conditions preserved both transcriptomes, as well as the GFP signal during the extended FACS procedure, while also sterilizing the sample (Extended Data Fig. 1e–h).

To assess coverage of pathogen and host transcripts, we first sequenced total RNA without further depletion or enrichment of certain RNA classes²¹, using Illumina technology. Of ~25 million RNA reads obtained from infected cells at 4 h, 98.2% were of human origin and 1.4% of *Salmonella* origin (Fig. 1b), confirming the predicted excess of eukaryotic over bacterial RNA¹⁵. Bacterial reads increased over time, reflecting intracellular replication of the pathogen (Fig. 1b; compare 4 and 24 h GFP⁺). Reads from *Salmonella* or HeLa cells alone mapped to their respective genomes with high stringency (Fig. 1b) and individual transcript levels were highly reproducible amongst biological triplicates (Extended Data Fig. 1i).

Collective sequencing of total RNA captured all major bacterial and eukaryotic transcript classes (Fig. 1b). Stable housekeeping ribosomal RNA (rRNA) transcripts were abundant in both transcriptomes, as were reads corresponding to transfer RNA (tRNA) in the *Salmonella* and stable small nucleic(ol)ar RNAs (snRNAs, snoRNAs) in the human transcriptome. Other noncoding bacterial RNA classes, that is, sRNAs and antisense transcripts, contributed ~8% of the *Salmonella* reads; the abundance of human regulatory noncoding transcripts ranged from 0.1% for the ~22 nucleotide-long microRNAs (miRNAs) to 15% for the 200 to 100,000 nucleotide-spanning long noncoding RNAs (lncRNAs).

Messenger RNAs, constituting 16–20% of all reads, predict differentially expressed proteins in both organisms during infection, which

¹University of Würzburg, RNA Biology Group, Institute for Molecular Infection Biology, Josef-Schneider-Straße 2/D15, D-97080 Würzburg, Germany. ²University of Würzburg, Core Unit Systems Medicine, Josef-Schneider-Straße 2/D15, D-97080 Würzburg, Germany. ³University of Leipzig, Department of Computer Science and Interdisciplinary Center for Bioinformatics, Härtelstraße 16-18, D-04107 Leipzig, Germany. ⁴University of Vienna, Theoretical Biochemistry Group, Institute for Theoretical Chemistry, Währinger Straße 17, A-1090 Vienna, Austria. ⁵Max Planck Genome Centre Cologne, Max Planck Institute for Plant Breeding Research, Carl-von-Linné-Weg 10, D-50829 Cologne, Germany. ⁶Max Planck Institute for Mathematics in the Sciences, Inselstraße 22, D-04103 Leipzig, Germany. ⁷Santa Fe Institute, 1399 Hyde Park Rd, Santa Fe, New Mexico 87501, USA. ⁸Research Centre for Infectious Diseases (ZINF), University of Würzburg, D-97070 Würzburg, Germany.

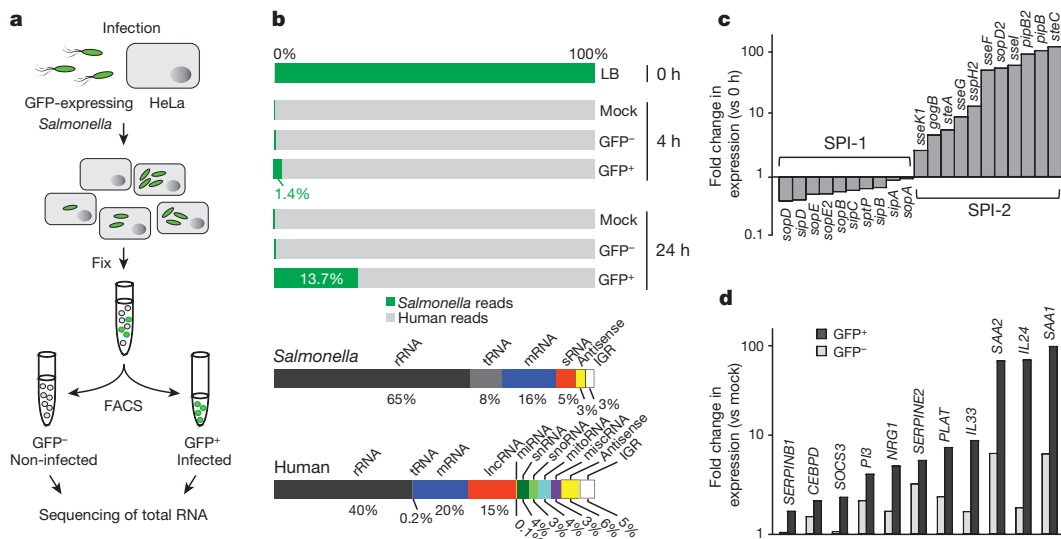


Figure 1 | Dual RNA-seq captures the full transcript repertoire of infected cells. **a**, Dual RNA-seq workflow. **b**, Representative mapping statistics from sorted *Salmonella*-infected HeLa-S3 cells. LB, *Salmonella* grown in medium. ‘miRNA’ includes primary and mature forms; ‘mitoRNA’ refers to mitochondrial transcripts. IGR, intergenic region;

was consistent with published pathogen²² and host²³ microarray data: expression of invasion-related genes of *Salmonella* pathogenicity island 1 (SPI-1) decreased after bacterial internalization, whereas expression of SPI-2 genes promoting intracellular survival increased (Fig. 1c). In invaded host cells, NF-κB-associated immunity genes were strongly activated (Fig. 1d). Thus, dual RNA-seq of mixed total RNA reliably profiled both coding and noncoding RNA patterns in intracellular bacteria and their host cells.

Dynamic sRNA expression in intracellular *Salmonella*

To increase coverage of informative transcripts and to make dual RNA-seq more sensitive, we successfully depleted both bacterial and eukaryotic rRNA (Extended Data Fig. 2). We then profiled sRNAs in intracellular *Salmonella* with high resolution, analysing time-course samples taken before and 2, 4, 8, 16 and 24 h after infection of HeLa cells (Extended Data Fig. 3a). Reads per kilobase transcript per million reads (RPKM) distributions revealed the relative abundance of bacterial and human RNA classes (Extended Data Fig. 3b). Altogether, we recorded expression of 145 known and 189 candidate *Salmonella* sRNAs, some of which were already induced greater than tenfold 2 h after invasion (Fig. 2a). Expression changes of well characterized sRNAs provided insight into *Salmonella*’s microenvironment inside the host, as exemplified by RyhB and IsrE which are activated following iron scarcity^{7,24} or MicA/L, RyhB and OmrA/B which all report bacterial surface stress^{25,26}. In addition, decreased SPI-1 and increased SPI-2 expression after bacterial internalization (see Fig. 1c) is reflected in co-transcriptionally regulated sRNAs: InvR and DapZ were repressed^{5,8}, whereas MgrR was activated²⁷.

The most activated sRNA, PinT (renamed from STnc440 (ref. 8) to PhoP-induced sRNA in intracellular *Salmonella*; see later) increased up to 100-fold during the infection, as well as in *Salmonella* grown in SPI-2-inducing medium which mimics the intracellular milieu²⁸ (Fig. 2a, b and Extended Data Fig. 3c). Likewise, PinT was prominently upregulated in dual RNA-seq experiments of 13 other host cell types, including murine bone marrow-derived macrophages, differentiated human THP-1 macrophages, and porcine macrophage-like cells (Fig. 2a, insets; Extended Data Fig. 4a, b).

PinT is an 80 nucleotide-long sRNA^{8,29} from a horizontally acquired *Salmonella*-specific locus that also encodes RtsA, a co-activator protein of invasion genes (Fig. 2c). However, a correlation analysis of all dual RNA-seq time points with global *Salmonella* regulons predicted

miscRNA, miscellaneous RNA. **c**, Compared to extracellular *Salmonella* (0 h), intracellular bacteria at 4 h p.i. repress SPI-1 and induce SPI-2 effector genes. **d**, Invaded (GFP⁺) host cells at 24 h p.i. activate NF-κB-associated immunity genes. Data in panels **c** and **d** represent fold changes calculated by edgeR over 3 biological replicates.

control by PhoP/Q (Fig. 2d), the SPI-2-activating two-component system that is essential for intracellular survival^{30,31}. Supporting this prediction, PinT expression was abrogated in a Δ PhoP strain and by mutations in the putative PhoP box in the *pinT* promoter (Extended Data Fig. 3d, e). Thus, PinT is a PhoP-dependent *Salmonella* sRNA that is highly activated upon infection of diverse host cells.

PinT sRNA times virulence mRNA expression

PinT exemplifies the current difficulty in understanding sRNA functions in bacterial virulence: an Hfq-bound sRNA of unknown function^{5,8,29}, PinT was selected as a potential *Salmonella* virulence factor in genome-wide random mutagenesis screens (TraDIS) in pigs and cattle¹³, two large-animal models of salmonellosis. Both its sequence conservation (Extended Data Fig. 3f) and its strong induction inside host cells further support a role for this sRNA in bacterial virulence. However, as the *pinT* gene was not selected by TraDIS in mice¹³ and its deletion produces weak macroscopic phenotypes in cultured cells (Extended Data Fig. 3g, h and Extended Data Fig. 4c–e), assays to decipher its molecular function during infection are currently lacking.

Combining several approaches, we discovered a molecular function of PinT as a timer of virulence gene expression, as summarized in Fig. 3a. First, a dual RNA-seq time-course using a Δ pinT strain to infect HeLa cells enabled the prediction that this sRNA represses SPI-2 genes during the early stages after host cell invasion (Fig. 3b and Extended Data Fig. 5a). The PinT-mediated repression of SPI-2 was independently validated for several transcripts for the secretion apparatus and effector proteins and by the rescue of wild-type expression profiles upon sRNA *trans*-complementation (strain pinT+) (Extended Data Fig. 5b). A dual RNA-seq time-course of *Salmonella*-infected cells from pigs, an organism in which PinT scored as a potential virulence factor¹³, also confirmed the PinT effect on SPI-2 (Fig. 3b and Extended Data Fig. 5a, c). Second, mRNA profiling suggested that PinT acts upstream of the SPI-2 master transcription factor, SsrB, without affecting its own activator PhoP/Q or the invasion gene regulator, Hld (Extended Data Fig. 5b). Third, we successfully recapitulated PinT-mediated repression of SPI-2 genes under defined *in vitro* conditions (Fig. 3b and Extended Data Fig. 5a).

We reasoned that as PinT associates with Hfq²⁹, it regulates mRNAs by base pairing³². To identify early-infection mRNA targets, we pulse-expressed PinT under pre-invasion conditions *in vitro* (Extended Data Fig. 6a and Supplementary Table 1). Two of

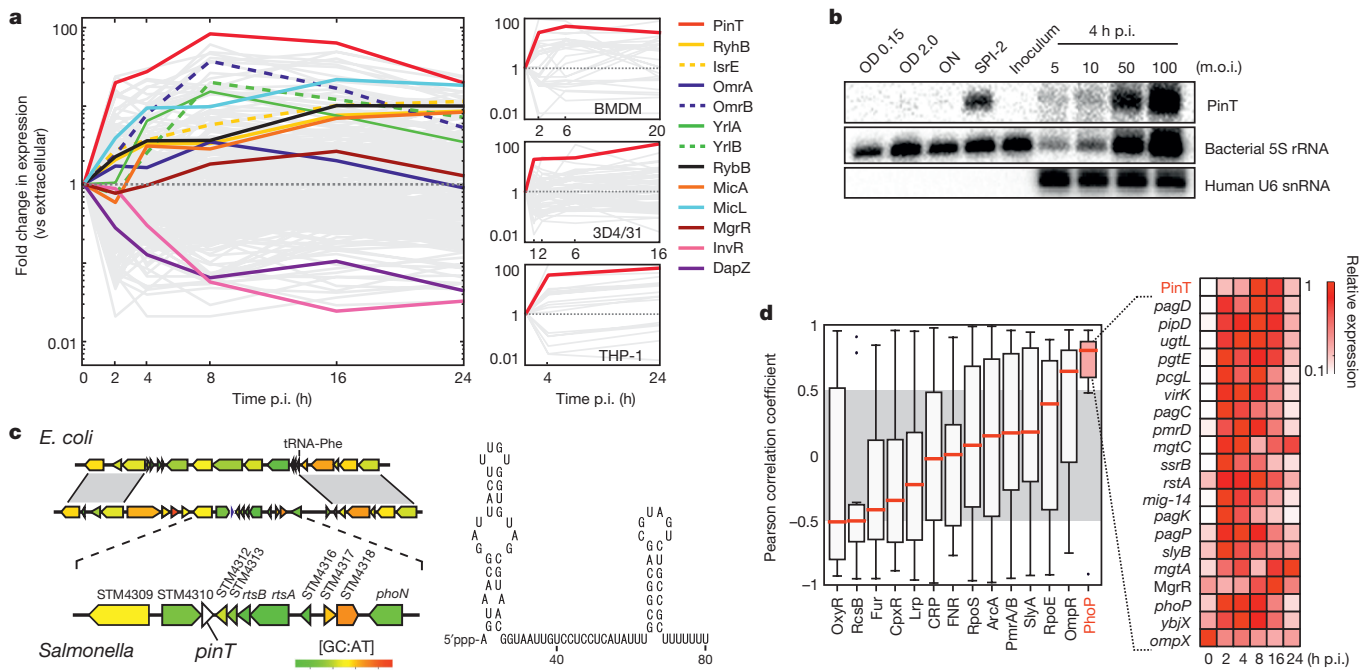


Figure 2 | A PhoP-dependent *Salmonella* sRNA induced inside host cells. **a**, Dual RNA-seq profiles of regulated *Salmonella* sRNAs in HeLa-S3 cells (adjusted P value < 0.05). Insets, PinT sRNA expression (red lines) in different macrophage-like cells. **b**, Northern blot detection of PinT. 5S and U6 RNAs represent loading controls. ON, overnight. ‘Inoculum’, bacteria in host cell medium before infection. Uncropped gel image in Supplementary Fig. 1. **c**, *pinT* locus and sRNA secondary structure.

the top repressed mRNAs encoded the secreted SPI-1 effectors SopE and SopE2. Conversely, the *sopE/E2* mRNAs were found to be de-repressed in Δ *pinT* *Salmonella* during host cell invasion (Extended Data Fig. 5b). SopE and SopE2 are guanidyl nucleotide exchange factors that stimulate innate immune responses³³ and contribute to the establishment of *Salmonella*’s replicative niche³⁴. They were readily depleted by overexpression of PinT, while other SPI-1 effectors such as SopB or SipC were unaffected (Fig. 3c), arguing for selective regulation. *In silico* modelling predicted that PinT base pairs near the start codon of the *sopE* and *sopE2* mRNAs, which was confirmed by compensatory mutations in *gfp* reporter constructs of these targets, and within the single-stranded ‘seed’ region of the sRNA (PinT* variant; Extended Data Fig. 6b, c).

To identify relevant PinT targets upon host cell entry, we successfully pulse-expressed PinT in bacteria growing inside host cells and also analysed PinT overexpression in the SPI-2-inducing medium (Extended Data Fig. 6d, e and Supplementary Table 1). The combined data sets enabled the prediction that PinT also directly represses the mRNAs encoding the proteins GrxA (glutathione/glutaredoxin system) and CRP (cyclic AMP receptor protein), by using the same seed sequence as above (Fig. 3c and Extended Data Fig. 6f).

As CRP and GrxA contribute to virulence gene activation in intracellular *Salmonella*^{35–37}, they might mediate PinT signalling to SPI-2. To address this, we monitored regulation of the well-known SsrB-activated SPI-2 gene *ssaG*²⁸ after a switch from SPI-1- to SPI-2-inducing media (Fig. 3d). This *in vitro* assay recapitulated the premature activation of SPI-2 previously seen in intracellular Δ *pinT* bacteria (Fig. 3b). Reciprocally, overexpression of PinT impaired SPI-2 gene activation. Importantly, this regulation was lost upon genomic deletion of *crp* but not of *grxA* (Fig. 3d), establishing the metabolic regulator CRP as a mediator of PinT control of SPI-2.

Together these data suggest that PinT shapes the transition from invasion to the intracellular replication state of *Salmonella* by simultaneously acting on two SPI-1 effectors and the SPI-2 virulence genes.

d, PinT as part of the PhoP regulon. Left, 14 analysed global regulons (Supplementary Table 1). Box plots show the interquartile range (IQR), with the median marked (red line). Whiskers indicate the highest/lowest point within $1.5 \times$ IQR of the upper/lower quartile. Right, expression of PhoP target genes during the course of infection. Sequencing data in panels **a** and **d** are derived from 3 biological replicates.

This model was supported with evidence at the protein level of an incomplete clearance of the SPI-1 effector SopE and a faster accumulation of SPI-2 effector SteC in the Δ *pinT* bacteria upon shifting from SPI-1 to SPI-2 conditions, as compared to PinT-expressing *Salmonella* (Fig. 3e). Intriguingly, although previous work discovered transcriptional loops that time SPI-2 expression³⁸, our study reveals that PinT provides a post-transcriptional repressor arm of PhoP in a complex feedback loop that helps *Salmonella* transit from SPI-1 to SPI-2 activity upon internalization (Fig. 3a, f). This makes PinT the first sRNA, to our knowledge, known to temporally shape the transition between two major bacterial virulence programs.

PinT impacts the host response

To understand how temporal virulence factor control by PinT may impact the host, we interrogated the dual RNA-seq time-course data for PinT-dependent changes in the transcriptomes of infected HeLa cells. Strikingly, wild-type and Δ *pinT* *Salmonella* elicit very different expression patterns amongst the 14,001 mRNAs, 3,982 lncRNAs and 134 miRNAs detected for the host (Fig. 4a and Extended Data Fig. 7a, b). Moreover, while PinT affects bacterial virulence gene expression early post-invasion of HeLa cells (Fig. 3b), its impact on the host transcriptome is apparent throughout the course of the infection (Fig. 4a); even before a small replication phenotype of the Δ *pinT* strain has manifested (Extended Data Fig. 3h).

Interspecies correlation analysis of pathogen and host transcriptome changes (see Methods) provided a potential molecular scenario of how PinT affects pathogen–host interplay by linking PinT-regulated SPI-2 gene expression in the bacteria with factors involved in the JAK–STAT pathway in the host (Fig. 4b and Supplementary Table 1). Specifically, we predicted and validated an accelerated activation of a key regulator of JAK–STAT signalling, Suppressor of cytokine signalling 3 (SOCS3), in the absence of PinT (Fig. 4a, c and Extended Data Fig. 7c). SOCS3 inhibits the phosphorylation of the STAT3 (signal transducers and activators of transcription 3) transcription factor to prevent its activation

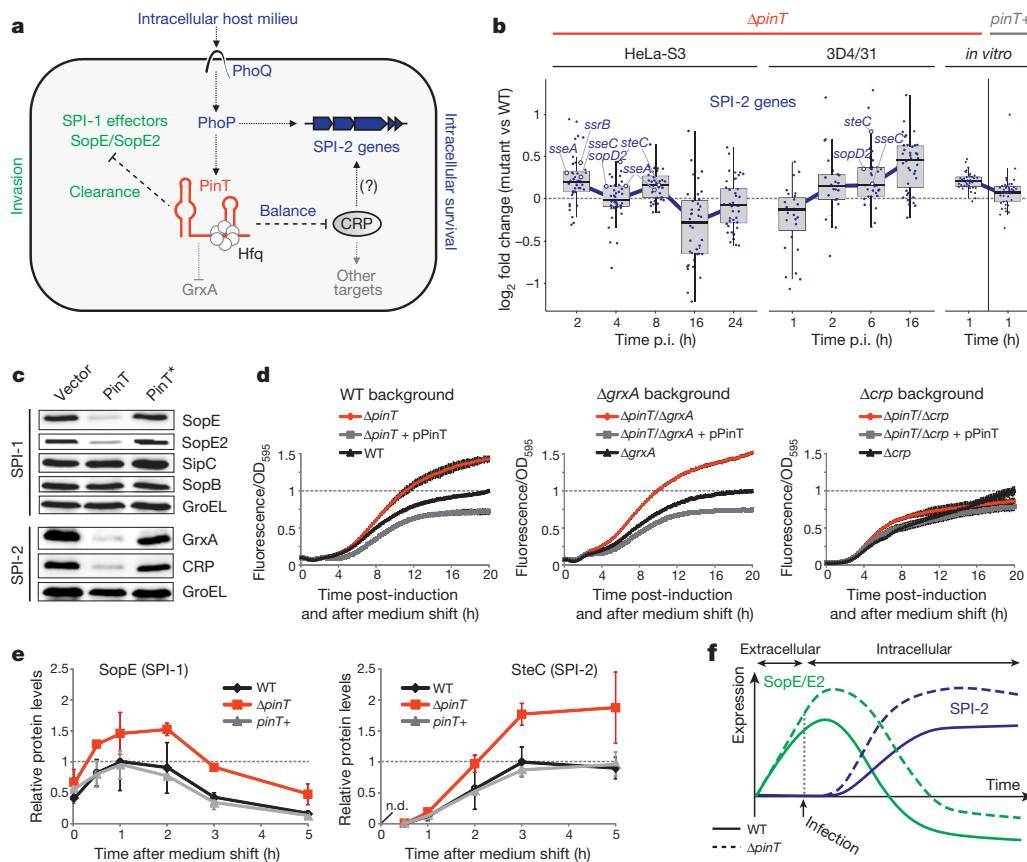


Figure 3 | PinT temporally controls *Salmonella* virulence genes. **a**, Model of virulence gene expression regulation by PinT (based on panels **b–e**). Green, SPI-1 branch; blue, SPI-2. **b**, Relative expression of SPI-2 genes between wild-type *Salmonella* and the ΔpinT or pinT^+ mutant strains. Box plots represent median expression fold changes of the regulon (whiskers: $1.5 \times \text{IQR}$ of the upper/lower quartile). Validated transcripts (Extended Data Fig. 5b, c) are labelled. **c**, Western blot analysis of PinT targets (identified in Extended Data Fig. 6). Overexpression of wild-type (PinT) or point-mutated (PinT*) sRNA under SPI-1 (LB, OD₆₀₀ = 2.0) or SPI-2 conditions (SPI-2 medium, OD₆₀₀ = 0.3). Empty vector and GroEL are negative and loading controls,

and nuclear import³⁹. Consistent with premature induction of SOCS3 (Fig. 4c), we observed reduced STAT3 phosphorylation in cells infected with ΔpinT *Salmonella* compared to wild-type infection (Fig. 4d).

Dual RNA-seq revealed additional impact of PinT activity on host immune pathways; for example, increased mRNA abundance of the pro-inflammatory chemokine interleukin 8 (*IL8*, also known as *CXCL8*) in HeLa cells infected with ΔpinT bacteria, which was further confirmed on both RNA and protein levels (Extended Data Fig. 7a, d, e). Interestingly, elevated *IL8* mRNA levels spread to bystander cells in ΔpinT -infected cultures (Extended Data Fig. 7d), probably due to paracrine immune signalling⁴⁰. Importantly, both PinT-controlled SPI-1 effectors SopE and SopE2, as well as several SPI-2 effectors influence JAK–STAT signalling or IL-8 secretion^{23,33,41,42}. These host responses are crucial for *Salmonella* to establish its intracellular replication niche²³ and compete with the intestinal microbiota^{43,44}, but also mediate bacterial killing⁴⁵. Therefore, our observations would favour a model in which *Salmonella* uses PinT-mediated temporal control of virulence genes for optimal manipulation of these key host cell pathways to promote its own replication.

Our dual RNA-seq data provides the first, to our knowledge, global map of both polyadenylated and non-polyadenylated host transcripts that respond to a bacterial infection (Extended Data Fig. 7a), providing a temporal view of infection-related lncRNA expression and processing. Intracellular *Salmonella* affect the levels of $\sim 44\%$ of all

respectively. Uncropped gel image in Supplementary Fig. 1. **d**, PinT represses SPI-2 through CRP. *Salmonella* strains with endogenous (black), ectopic (grey) or lacking PinT expression (red) in either wild-type or deletion background were shifted from SPI-1 to SPI-2 conditions (see Methods). A transcriptional reporter fusion of the SPI-2 gene *ssaG* to *gfp* was used as a proxy for SPI-2 induction. **e**, Western blot quantification of *sopE::flag/steC::flag* *Salmonella* shifted from SPI-1 to SPI-2 conditions. Protein levels were normalized to GroEL. Points and error bars indicate the mean \pm s.d. from 3 biological replicates. n.d., not detected. **f**, Model of the temporal expression of virulence genes in the presence or absence of PinT.

detected lncRNAs throughout the genome, almost half of which differ between wild-type and ΔpinT infections (Fig. 4a and Extended Data Fig. 7a, b, f). Remarkably, certain lncRNAs appear to respond very quickly to PinT-dependent alterations (Fig. 4a), suggesting that lncRNAs can provide sensitive markers for pathogen activities in the early infection phase.

Dual RNA-seq further permits the analysis of alternative splicing events, the formation of circular RNAs, and expression changes in small open reading frames; however, PinT generally had little, if any, impact on these processes (data not shown). However, in addition to pathogen and nuclear host transcripts, our protocol readily captures non-polyadenylated organellar transcripts (Fig. 1b), revealing that *Salmonella* strongly induces mitochondrial gene expression in invaded host cells (Extended Data Fig. 7a). Moreover, the ΔpinT strain caused hyperactivation of global mitochondrial RNA expression including the mitochondrial oxidative phosphorylation pathway and altered the subcellular localization of mitochondria (Fig. 4a, e and Extended Data Fig. 8). Although the underlying molecular mechanisms remain to be determined, these findings illustrate how a single sRNA affects host–pathogen interactions at different levels (Fig. 4f). Importantly, the combined data exemplifies how the generic analysis of all transcript classes by dual RNA-seq can reveal changes at the cellular level to provide molecular insight into the roles of genes identified in pathogenesis screens using animal models.

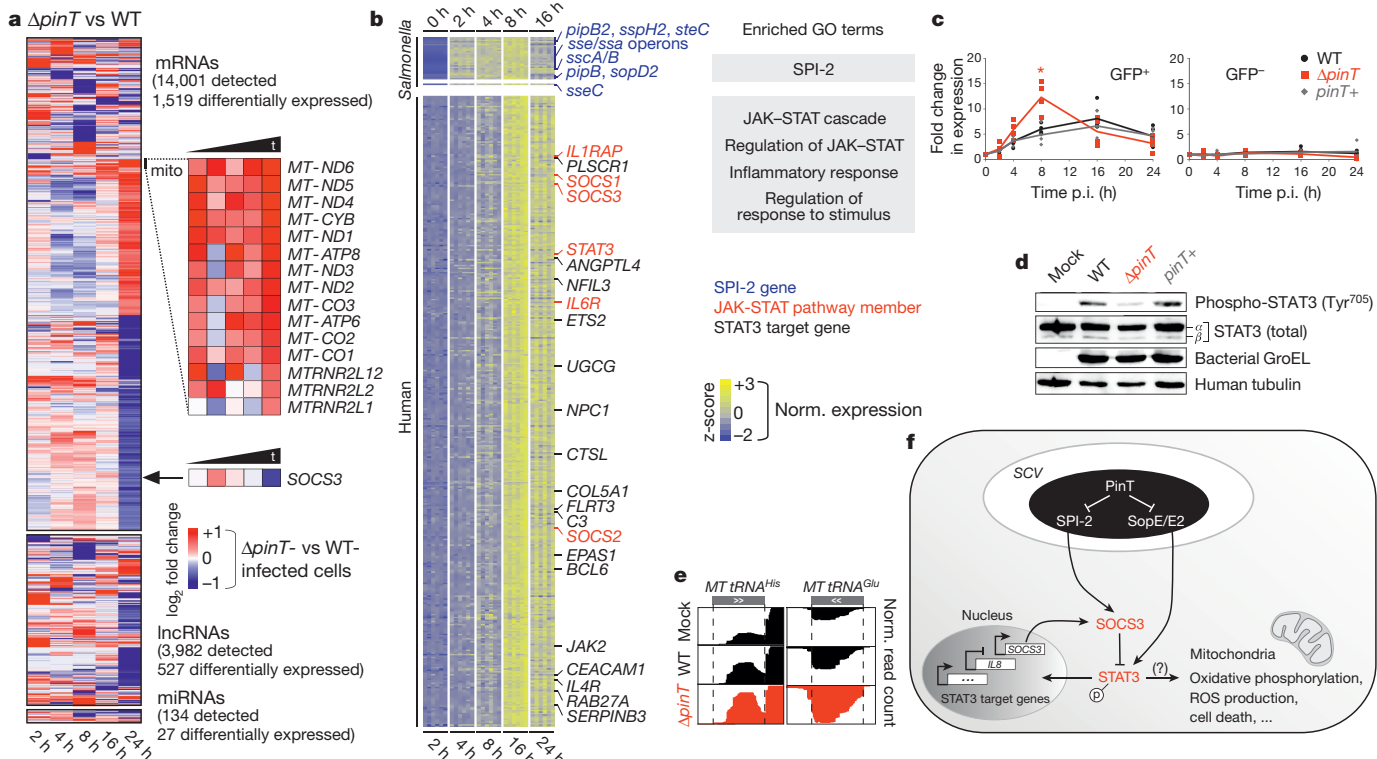


Figure 4 | Effect of PinT activity on the host transcriptome.

a, Differentially expressed HeLa-S3 transcripts (adjusted P value < 0.05 ; 3 biological replicates) between wild-type and ΔpinT infections. Numbers reflect detected and differentially expressed transcripts, respectively. Full gene lists are in Supplementary Table 1. **b**, Interspecies co-regulation analysis (see Methods) correlates *Salmonella* SPI-2 genes with the human JAK-STAT pathway. Enriched bacterial and human GO terms are displayed. Complete gene sets in Supplementary Table 1. **c**, qRT-PCR measurements of human SOCS3 mRNA in infected (GFP⁺) and bystander (GFP⁻) HeLa-S3 cells after wild-type, ΔpinT or pinT^+ infection. Data represent results from 3 (2 h) or 4 (other time points) biological replicates,

asterisk denotes significant expression differences between wild-type- and ΔpinT -infected cells ($P < 0.05$; one-tailed Mann-Whitney U -test). **d**, Western blot of phosphorylation status of STAT3 in unsorted HeLa-S3 cells at 16 h p.i. with the indicated strains, including bacterial (GroEL) and human (tubulin) loading controls. Uncropped gel image in Supplementary Fig. 1. **e**, Representative dual RNA-seq coverage plot for two mitochondrial tRNA genes at 16 h p.i. of HeLa-S3. **f**, Summary of how PinT-dependent regulation of bacterial effectors that affect SOCS3 (ref. 41) or, via Rho-GTPases, STAT3 (ref. 23), may influence host JAK-STAT signalling. STAT3 also affects mitochondria⁵⁰, which potentially interconnects the different PinT-affected host pathways. SCV, *Salmonella*-containing vacuole.

Outlook

Using dual RNA-seq, we have comprehensively charted the dynamic RNA expression landscape of both a bacterial pathogen and its eukaryotic host during the course of infection. This approach enabled us to discover PinT as a post-invasion-activated sRNA whose function in host-pathogen interactions manifests itself in pervasive expression changes in all classes of host RNA. Many other sRNA loci are strongly induced upon host cell invasion (Fig. 2a). We selected six whose *in vivo* induction was recapitulated in SPI-2 medium (Extended Data Fig. 9a) for pairwise genomic inactivation. Of these, OmrA/B and RyhB/IsrE each control multiple mRNAs by Hfq-dependent base pairing^{24,26,46}, while YrlA/B program RNA decay in *Salmonella*⁴⁷. Whereas none of the $\Delta\text{omrA}/\Delta\text{omrB}$, $\Delta\text{ryhB}/\Delta\text{isrE}$, and $\Delta\text{yrlA}/\Delta\text{yrlB}$ deletion strains displayed a phenotype in standard invasion/replication assays (Extended Data Fig. 9b, c), initial dual RNA-seq of HeLa cells infected with these double mutants revealed strain-specific changes in *Salmonella* transcripts (Extended Data Fig. 9d, e) and differential pathway activities in infected host cells (Extended Data Fig. 9f, g). While certain host pathways were generically de-regulated by all three mutants (Extended Data Fig. 9g), other pathways were specifically impacted by distinct deletion strains, suggesting that *Salmonella* sRNAs actively contribute to successful host infection by affecting common as well as disparate host pathways.

Virulence factor screens have identified many *Salmonella* protein-coding and sRNA genes whose molecular contributions to successful infection have remained unknown due to a failure to link a phenotype to its underlying mechanism^{12–14,48,49}. Our findings with

PinT and other intracellularly induced sRNAs illustrate how small perturbations in the infection process, such as dysregulation of a few *Salmonella* mRNAs, can propagate through the entire host system, potentially leading to different disease outcomes in the context of a whole organism. The one-step nature of dual RNA-seq should enable high-throughput studies to unravel such hidden gene functions simultaneously in the pathogen and host, during infection with *Salmonella* and many other pathogens.

Online Content Methods, along with any additional Extended Data display items and Source Data, are available in the online version of the paper; references unique to these sections appear only in the online paper.

Received 8 August 2014; accepted 18 December 2015.

Published online 20 January 2016.

1. Caldelari, I., Chao, Y., Romby, P. & Vogel, J. RNA-mediated regulation in pathogenic bacteria. *Cold Spring Harb. Perspect. Med.* **3**, http://dx.doi.org/10.1101/cshperspect.a010298 (2013).
2. Gottesman, S. & Storz, G. Bacterial small RNA regulators: versatile roles and rapidly evolving variations. *Cold Spring Harbor Perspect. Biol.* **3**, http://dx.doi.org/10.1101/cshperspect.a003798 (2011).
3. Wagner, E. G. & Romby, P. Small RNAs in Bacteria and Archaea: who they are, what they do, and how they do it. *Adv. Genet.* **90**, 133–208 (2015).
4. Kroger, C. et al. An infection-relevant transcriptomic compendium for *Salmonella enterica* serovar Typhimurium. *Cell Host Microbe* **14**, 683–695 (2013).
5. Chao, Y., Papenfort, K., Reinhardt, R., Sharma, C. M. & Vogel, J. An atlas of Hfq-bound transcripts reveals 3' UTRs as a genomic reservoir of regulatory small RNAs. *EMBO J.* **31**, 4005–4019 (2012).
6. Ortega, A. D., Gonzalo-Asensio, J. & Garcia-del Portillo, F. Dynamics of *Salmonella* small RNA expression in non-growing bacteria located inside eukaryotic cells. *RNA Biol.* **9**, 469–488 (2012).

7. Padalon-Brauch, G. et al. Small RNAs encoded within genetic islands of *Salmonella typhimurium* show host-induced expression and role in virulence. *Nucleic Acids Res.* **36**, 1913–1927 (2008).
8. Pfeiffer, V. et al. A small non-coding RNA of the invasion gene island (SPI-1) represses outer membrane protein synthesis from the *Salmonella* core genome. *Mol. Microbiol.* **66**, 1174–1191 (2007).
9. Gong, H. et al. A *Salmonella* small non-coding RNA facilitates bacterial invasion and intracellular replication by modulating the expression of virulence factors. *PLoS Pathog.* **7**, e1002120 (2011).
10. Papenfort, K., Podkaminski, D., Hinton, J. C. & Vogel, J. The ancestral SgrS RNA discriminates horizontally acquired *Salmonella* mRNAs through a single G-U wobble pair. *Proc. Natl Acad. Sci. USA* **109**, E757–E764 (2012).
11. Sittka, A., Pfeiffer, V., Tedin, K. & Vogel, J. The RNA chaperone Hfq is essential for the virulence of *Salmonella typhimurium*. *Mol. Microbiol.* **63**, 193–217 (2007).
12. Santiviago, C. A. et al. Analysis of pools of targeted *Salmonella* deletion mutants identifies novel genes affecting fitness during competitive infection in mice. *PLoS Pathog.* **5**, e1000477 (2009).
13. Chaudhuri, R. R. et al. Comprehensive assignment of roles for *Salmonella* Typhimurium genes in intestinal colonization of food-producing animals. *PLoS Genetics* **9**, e1003456 (2013).
14. Barquist, L. & Vogel, J. Accelerating discovery and functional analysis of small RNAs with new technologies. *Annu. Rev. Genet.* **49**, 367–394 (2015).
15. Westermann, A. J., Gorski, S. A. & Vogel, J. Dual RNA-seq of pathogen and host. *Nature Rev. Microbiol.* **10**, 618–630 (2012).
16. Sorek, R. & Cossart, P. Prokaryotic transcriptomics: a new view on regulation, physiology and pathogenicity. *Nature Rev. Genet.* **11**, 9–16 (2010).
17. Humphrys, M. S. et al. Simultaneous transcriptional profiling of bacteria and their host cells. *PLoS ONE* **8**, e80597 (2013).
18. Malik-Kale, P. et al. *Salmonella*—at home in the host cell. *Front. Microbiol.* **2**, 125 (2011).
19. Wyllie, D. H. et al. Evidence for an accessory protein function for Toll-like receptor 1 in anti-bacterial responses. *J. Immunol.* **165**, 7125–7132 (2000).
20. Burnmann, D. Examination of *Salmonella* gene expression in an infected mammalian host using the green fluorescent protein and two-colour flow cytometry. *Mol. Microbiol.* **43**, 1269–1283 (2002).
21. Sharma, C. M. et al. The primary transcriptome of the major human pathogen *Helicobacter pylori*. *Nature* **464**, 250–255 (2010).
22. Hautefort, I. et al. During infection of epithelial cells *Salmonella enterica* serovar Typhimurium undergoes a time-dependent transcriptional adaptation that results in simultaneous expression of three type 3 secretion systems. *Cell Microbiol.* **10**, 958–984 (2008).
23. Hannemann, S., Gao, B. & Galan, J. E. *Salmonella* modulation of host cell gene expression promotes its intracellular growth. *PLoS Pathog.* **9**, e1003668 (2013).
24. Masse, E., Vanderpool, C. K. & Gottesman, S. Effect of RyhB small RNA on global iron use in *Escherichia coli*. *J. Bacteriol.* **187**, 6962–6971 (2005).
25. Guo, M. S. et al. MicL, a new σE-dependent sRNA, combats envelope stress by repressing synthesis of Lpp, the major outer membrane lipoprotein. *Genes Dev.* **28**, 1620–1634 (2014).
26. Guillier, M. & Gottesman, S. The 5' end of two redundant sRNAs is involved in the regulation of multiple targets, including their own regulator. *Nucleic Acids Res.* **36**, 6781–6794 (2008).
27. Moon, K., Six, D. A., Lee, H. J., Raetz, C. R. & Gottesman, S. Complex transcriptional and post-transcriptional regulation of an enzyme for lipopolysaccharide modification. *Mol. Microbiol.* **89**, 52–64 (2013).
28. Löber, S., Jackel, D., Kaiser, N. & Hensel, M. Regulation of *Salmonella* pathogenicity island 2 genes by independent environmental signals. *Int. J. Med. Microbiol.* **296**, 435–447 (2006).
29. Sittka, A. et al. Deep sequencing analysis of small noncoding RNA and mRNA targets of the global post-transcriptional regulator, Hfq. *PLoS Genet.* **4**, e1000163 (2008).
30. Prost, L. R., Daley, M. E., Bader, M. W., Klevit, R. E. & Miller, S. I. The PhoQ histidine kinases of *Salmonella* and *Pseudomonas* spp. are structurally and functionally different: evidence that pH and antimicrobial peptide sensing contribute to mammalian pathogenesis. *Mol. Microbiol.* **69**, 503–519 (2008).
31. Groisman, E. A. The pleiotropic two-component regulatory system PhoP-PhoQ. *J. Bacteriol.* **183**, 1835–1842 (2001).
32. Vogel, J. & Luisi, B. Hfq and its constellation of RNA. *Nature Rev. Microbiol.* **9**, 578–589 (2011).
33. Bruno, V. M. et al. *Salmonella* Typhimurium type III secretion effectors stimulate innate immune responses in cultured epithelial cells. *PLoS Pathog.* **5**, e1000538 (2009).
34. Vonaesch, P. et al. The *Salmonella* Typhimurium effector protein SopE transiently localizes to the early SCV and contributes to intracellular replication. *Cell. Microbiol.* **16**, 1723–1735 (2014).
35. Bjur, E., Eriksson-Ygberg, S., Aslund, F. & Rhen, M. Thioredoxin 1 promotes intracellular replication and virulence of *Salmonella enterica* serovar Typhimurium. *Infect. Immun.* **74**, 5140–5151 (2006).
36. Chen, Z. W. et al. Mutations in the *Salmonella enterica* serovar Choleraesuis cAMP-receptor protein gene lead to functional defects in the SPI-1 type III secretion system. *Vet. Res.* **41**, 05 (2010).
37. Yoon, H. J., McDermott, J. E., Porwollik, S., McClelland, M. & Heffron, F. Coordinated regulation of virulence during systemic infection of *Salmonella enterica* serovar Typhimurium. *PLoS Pathogens* **5**, e1000306 (2009).
38. Choi, J. & Groisman, E. A. The lipopolysaccharide modification regulator PmrA limits *Salmonella* virulence by repressing the type three-secretion system Spi/Ssa. *Proc. Natl Acad. Sci. USA* **110**, 9499–9504 (2013).
39. Li, Y., de Haar, C., Peppelenbosch, M. P. & van der Woude, C. J. SOCS3 in immune regulation of inflammatory bowel disease and inflammatory bowel disease-related cancer. *Cytokine Growth Factor Rev.* **23**, 127–138 (2012).
40. Browning, D. D., Diehl, W. C., Hsu, M. H., Schraufstatter, I. U. & Ye, R. D. Autocrine regulation of interleukin-8 production in human monocytes. *Am. J. Physiol. Lung Cell. Mol. Physiol.* **279**, L1129–L1136 (2000).
41. Uchiya, K. & Nikai, T. *Salmonella* pathogenicity island 2-dependent expression of suppressor of cytokine signaling 3 in macrophages. *Infect. Immun.* **73**, 5587–5594 (2005).
42. Bhavsar, A. P. et al. The *Salmonella* type III effector SspH2 specifically exploits the NLR co-chaperone activity of SGT1 to subvert immunity. *PLoS Pathog.* **9**, e1003518 (2013).
43. Winter, S. E. et al. Gut inflammation provides a respiratory electron acceptor for *Salmonella*. *Nature* **467**, 426–429 (2010).
44. Stecher, B. et al. *Salmonella enterica* serovar Typhimurium exploits inflammation to compete with the intestinal microbiota. *PLoS Biol.* **5**, e244 (2007).
45. Gewirtz, A. T., Siber, A. M., Madara, J. L. & McCormick, B. A. Orchestration of neutrophil movement by intestinal epithelial cells in response to *Salmonella* typhimurium can be uncoupled from bacterial internalization. *Infect. Immun.* **67**, 608–617 (1999).
46. Holmqvist, E. et al. Two antisense RNAs target the transcriptional regulator CsgD to inhibit curli synthesis. *EMBO J.* **29**, 1840–1850 (2010).
47. Chen, X. et al. An RNA degradation machine sculpted by Ro autoantigen and noncoding RNA. *Cell* **153**, 166–177 (2013).
48. Mazurkiewicz, P., Tang, C. M., Boone, C. & Holden, D. W. Signature-tagged mutagenesis: barcoding mutants for genome-wide screens. *Nature Rev. Genet.* **7**, 929–939 (2006).
49. Becker, D. et al. Robust *Salmonella* metabolism limits possibilities for new antimicrobials. *Nature* **440**, 303–307 (2006).
50. Myers, M. G. Moonlighting in mitochondria. *Science* **323**, 723–724 (2009).

Supplementary Information is available in the online version of the paper.

Acknowledgements We thank S. Gorski for help with the manuscript, C. Sharma and A. Eulalio for comments on the paper and L. Pfeuffer, B. Plaschke and V. McParland for technical assistance. We further thank S. Hoffmann for discussions about bioinformatic analyses, T. Rudel, K. Tedin, T. Meyer and C. Sharma for eukaryotic cell lines, V. Kozjak-Pavlovic for MitoTracker orange dye, T. Strowig for Ribo-Zero reagents, and W.-D. Hardt, M. Kolbe, H. Aiba and A. Eulalio for providing primary antibodies. A.J.W. was the recipient of an Elite Advancement Ph.D. stipend from the Universität Bayern e.V., Germany. L.B. is supported by a research fellowship from the Alexander von Humboldt Stiftung/Foundation. The Vogel laboratory received funding from the Bavarian BioSysNet program and BMBF (Bundesministerium für Bildung und Forschung) grant “Next-generation transcriptomics of bacterial infections”. This work was further supported by a donation from Baldwin Knauf to the Research Center for Infectious Diseases (ZIN). J.V. and P.F.S. acknowledge support by a joint BMBF grant eBio:RNAs. This work used the European Grid Infrastructure (EGI) and funding by the EGI-Engage project (Horizon 2020) under grant number 654142.

Author Contributions A.J.W., Y.C., L.N.S. and J.V. designed the research; A.J.W., Y.C. and L.N.S. performed the bench laboratory work; K.U.F., F.A., L.B., L.M. and P.F.S. conducted computational analyses; R.R. carried out part of the sequencing; A.J.W. and J.V. wrote the manuscript, which all co-authors commented on. J.V. supervised the project.

Author Information All RNA-seq data has been deposited in NCBI's Gene Expression Omnibus under accession number GSE60144. Reprints and permissions information is available at www.nature.com/reprints. The authors declare no competing financial interests. Readers are welcome to comment on the online version of the paper. Correspondence and requests for materials should be addressed to J.V. (joerg.vogel@uni-wuerzburg.de).

METHODS

Data reporting. No statistical methods were used to predetermine sample size. The investigators were not blinded to allocation during experiments and outcome assessment.

Salmonella strains and mammalian cell lines. *Salmonella enterica* serovar Typhimurium strain SL1344 constitutively expressing GFP from a chromosomal locus (strain JVS-3858) was previously described⁵¹ and is referred to as wild type throughout this study. The complete list of bacterial strains used in this study is provided in Supplementary Table 1. Routinely, bacteria were grown in Lennox broth (LB) medium at 37 °C with shaking at 220 r.p.m. When appropriate, 100 µg ml⁻¹ ampicillin (Amp), 50 µg ml⁻¹ kanamycin (Kan), or 20 µg ml⁻¹ chloramphenicol (Cm) (final concentrations) were added to the liquid medium or agar plates. Chromosomal mutagenesis of *Salmonella* SL1344 was performed as previously described⁵². To construct a non-polar *pinT* mutant strain (YCS-034, GFP⁻; or JVS-10038, GFP⁺), the first ~60 nt of the gene were removed and replaced by a resistance cassette, while keeping the Rho-independent terminator intact. Then, the resistance cassette was eliminated using the FLP helper plasmid pCP20 at 42 °C⁵². All mutations were transduced into the wild-type background using P22 phage⁵³. For plasmid transformation the respective *Salmonella* strains were electroporated with ~10 ng of DNA.

The following cell lines were used in this study: human cervix carcinoma cells (HeLa-S3; ATCC CCL-2.2), human epithelial colorectal adenocarcinoma cells (CaCo-2; ATCC HTB-37), human epithelial colorectal adenocarcinoma cells (HT29; DSMZ No. ACC-299), human stomach adenocarcinoma cells (AGS; ATCC CRL-1739), human epithelial colon metastatic cells (LoVo; ATCC CCL-229), human embryonic kidney 293 cells (HEK293; ATCC CRL-1573), human monocytic cells (THP-1; ATCC TIB-202), murine fibroblast cells (L929; ATCC CCL-1), murine embryonic fibroblast cells (MEF; ATCC SCRC-1040), mouse leukaemic monocyte/macrophage cells (RAW264.7; ATCC TIB-71), porcine intestinal epithelial cells (IPEC-J2)⁵⁴, porcine macrophage-like cells (3D4/31)⁵⁵.

HeLa-S3, CaCo-2, THP-1, HEK293; RAW264.7 and MEF cells were obtained from the group of Thomas Rudel (Biocentre, Würzburg). AGS cells were provided by Cynthia Sharma (Research Center for Infectious Diseases, Würzburg). L929 cells were obtained from Thomas Meyer (Max Planck Institute for Infection Biology, Berlin). HT29, LoVo, IPEC-J2 and 3D4/31 cells were provided by Karsten Tedin (Centre for Infection Medicine, Berlin). Cell lines have not been authenticated in our laboratory, but were routinely tested for mycoplasma contamination (MycoAlert Mycoplasma Detection Kit, Lonza).

HeLa-S3 cells were cultured according the guidelines provided by the ENCODE consortium (http://genome.ucsc.edu/encode/protocols/cell/human/Stam_15_protocols.pdf). Briefly, cells were grown in DMEM (Gibco) supplemented with 10% fetal calf serum (FCS; Biochrom), 2 mM L-glutamine (Gibco) and 1 mM sodium pyruvate (Gibco) in T-75 flasks (Corning) in a 5% CO₂, humidified atmosphere, at 37 °C. Further cell lines used in this study (THP-1, CaCo-2, AGS, HT29, LoVo, HEK293, MEF, L929, RAW264.7, IPEC-J2 and 3D4/31) were cultured in RPMI (Gibco) supplemented with 10% FCS, 2 mM L-glutamine, 1 mM sodium pyruvate and 0.5% β-mercaptoethanol (Gibco) in a 5% CO₂, humidified atmosphere, at 37 °C. To differentiate THP-1 monocytes, seeded cells (1 × 10⁶ cells per well; six-well format) were treated with 50 ng ml⁻¹ (final concentration) of phorbol 12-myristate 13-acetate (PMA) (Sigma) for 72 h (after 48 h fresh PMA at the same concentration was added to the culture).

For the differentiation of murine bone marrow derived macrophages (BMDMs), the marrow of femur and tibia was isolated from 8–12-week-old female C57BL/6 wild-type mice and stored in RPMI supplemented with 10% FCS. The cell suspension was centrifuged for 5 min at 250g and the leukocyte pellet was resuspended in differentiation medium consisting of X-vivo-15 medium (Lonza) supplemented with 10% FCS and 10% L929-conditioned DMEM medium (same composition as above). Cells were cultured at 3 × 10⁶ cells per 10 ml in a T-75 flask. At day 3, another 3 ml of differentiation medium were added and cells were further cultured until day 5. Successful macrophage differentiation was validated by microscopy before the cells were detached using a rubber scraper (Sarstedt) and seeded into six-well plates at 10⁵ cells per well in fresh differentiation medium. Infection was carried out on day 7 as described below.

Salmonella infection assay. *In vitro* infection of HeLa-S3 cells was carried out following a previously published protocol⁵⁶ with slight modifications. Two days before infection 2 × 10⁵ HeLa-S3 cells were seeded in 2 ml complete DMEM (six-well format). Overnight cultures of *Salmonella* were diluted 1:100 in fresh LB medium and grown aerobically to an OD₆₀₀ of 2.0. Bacterial cells were harvested by centrifugation (2 min at 12,000 r.p.m., room temperature) and resuspended in DMEM. Infection of HeLa-S3 cells was carried out by adding the bacterial suspension directly to each well. If not mentioned otherwise, infections were performed at a multiplicity of infection (m.o.i.) of 5. Immediately after addition of bacteria, the plates were centrifuged for 10 min at 250g at room temperature followed by

30 min incubation in 5% CO₂, humidified atmosphere, at 37 °C. Medium was then replaced for gentamicin-containing DMEM (final concentration: 50 µg ml⁻¹) to kill extracellular bacteria. After a further 30 min incubation step, medium was again replaced by fresh DMEM containing 10 µg ml⁻¹ of gentamicin, and incubated for the remainder of the experiment. Time point 0 was defined as the time when gentamicin was first added to the cells.

Further cell types were infected as described for HeLa-S3 cells except that infection was carried out in RPMI medium and that infection was with an m.o.i. of 10 (THP-1, CaCo-2, HT29, AGS, HEK293, MEF, L929 and RAW264.7) or 20 (IPEC-J2, 3D4/31), respectively. Infection of BMDMs was carried out with an m.o.i. of 10 and using X-vivo-15 medium (10% fetal calf serum, 10% L929-conditioned medium).

Confocal laser scanning microscopy. Infection was carried out as described above, except that HeLa-S3 cells had been seeded onto coverslips (24-well format). At the respective timepoint, coverslips with infected HeLa-S3 were washed twice with PBS (Gibco) and fixed in 4% paraformaldehyde (PFA) for 15 min in a wet chamber. After two additional PBS washing steps, cells were stained with Hoechst 33342 (Invitrogen; diluted 1:5,000 in PBS) for 15 min in a wet chamber and again washed twice with PBS. After coverslips had been air-dried, they were embedded in Vectashield Mounting Medium (Biozol) and analysed using the Leica SP5 confocal microscope (Leica) and the LAS AF Lite software (Leica).

To stain human mitochondria, MitoTracker Orange CMTMRos (Life Technologies; kindly provided by V. Kozjak-Pavlovic, Biocentre, Würzburg) was used. The dye was added in the dark to a final concentration of 200 nM directly into the medium of the infected cells in the 37 °C incubator, 30 min before their harvest. After the 30 min incubation with the dye, the plates were covered with aluminium foil to prevent bleaching during the following steps. The supernatant was aspirated and the cells were washed with PBS and fixed with 4% PFA at 4 °C overnight. Hoechst staining and sample preparation was performed as described above.

Flow cytometry and fluorescence-activated cell sorting (FACS). For flow cytometry-based analyses, infected cultures were washed twice with PBS, detached from the bottom of the plate by trypsinization and resuspended in complete DMEM. Upon pelleting the cells (5 min at 250g, room temperature), they were resuspended in PBS and analysed by flow cytometry using a FACSCalibur instrument (BD Biosciences) and the Cyflogic (CyFlo Ltd; version 1.2.1) or Flowing (Cell Imaging Core, Turku Centre for Biotechnology, Finland; version 2.5.0) software, respectively. Selection of intact HeLa-S3 cells was achieved by gating based on cell diameter (forward-scatter) and granularity (side-scatter) (linear scale). Of those, infected (GFP-positive) and non-infected (GFP-negative) sub-fractions were defined based on GFP signal intensity (FITC channel) versus auto-fluorescence (PE channel) (logarithmic scale).

For cell sorting, RNA/*later*-fixed cells (see below) were first passed through MACS Pre-Separation Filters (30 µm exclusion size; Miltenyi Biotec) and then analysed and sorted using the FACSAria III device (BD Biosciences) at 4 °C (cooling both the input tube holder and the collection tube rack) and at a medium flow rate using the same gating strategy as described above, except that the gates for GFP-positive and GFP-negative fractions were conservative in order to prevent cross-contamination (as exemplified in Extended Data Fig. 1d). Typically ~2 × 10⁵ cells of each fraction were collected for RNA isolation.

Staining of apoptotic cells and cytotoxicity assay. To detect apoptotic cells, HeLa-S3 cells were washed twice with PBS and resuspended in 1 × binding buffer (BD Pharmingen) to a concentration of 10⁶ cells per ml. 100 µl of this cell suspension were mixed with 5 µl of APC-labelled annexin V (BD Pharmingen) and 1 µl of 500 mg ml⁻¹ propidium iodide (PI; lyophilized stock from Sigma). Upon incubation for 15 min at room temperature, (light-protected) cells were subjected to flow cytometry using the MACSQuant Analyzer (Miltenyi Biotec). Upon gating of the fraction of intact cells based on cell diameter (forward-scatter) and granularity (side-scatter), the annexin-positive/PI-negative sub-population was determined by comparison against the appropriate single-stained controls in the APC vs PerCP channels, and quantified.

Necrosis was evaluated by quantifying released lactate dehydrogenase (LDH) via the Cytotox96 assay (Promega) according to the manufacturer's instructions. The absorbance at 490 nm was measured using a Multiskan Ascent instrument (Thermo Fisher). In order to convert the measured absorbance values into the relative proportion of dead cells, the maximal absorbance was determined by using 1 × lysis solution (Promega) following the manufacturer's instructions and referred to as 100% cytotoxicity. For both apoptosis and cytotoxicity measurements each biological replicate comprised three technical replicates.

Quantification of intracellular replication (flow cytometry, c.f.u. assay). To quantify bacterial intracellular replication (Extended Data Fig. 1b), infected host cells were analysed by flow cytometry as described above, except that the increase in GFP intensity (geometric mean) was measured in the GFP-positive

sub-population over time and normalized to that of the non-infected population in the same sample (example in Extended Data Fig. 1c).

Alternatively, infected HeLa-S3 cultures were solubilized with PBS containing 0.1% Triton X-100 (Gibco) at the respective time points. Cell lysates were serially diluted in PBS, plated onto LB plates and incubated at 37 °C overnight. The number of colony forming units (c.f.u.) recovered was compared to that obtained from the bacterial input solution used for infection. In all cases, each biological replicate comprised three technical replicates.

Evaluation of different fixation techniques. Infected cells were washed twice with PBS, trypsinized and pelleted. For ethanol fixations, cell pellets were re-dissolved in 0.1 volume of ice-cold PBS and then 0.9 volume of ice-cold ethanol (either 70% or 100%; as indicated) were added in single droplets during shaking (400 r.p.m., 4 °C) to avoid cell clumping. Fixation using stop solution (95% EtOH/5% water-saturated phenol)⁵⁷ was performed by resuspending the cell pellet in PBS before the addition of 0.2 volume of stop solution and mixing. When PFA was used, the pellet was resuspended in the respective PFA concentration (0.5% or 4% PFA, pH 7.4, with or without 4% sucrose) and shaken for 15 min at 400 r.p.m., room temperature. PFA-induced crosslinks were reverted by an additional heating step for 15 min at 70 °C (refs 58, 59). For fixation with RNAlater (Qiagen), cell pellets were directly resuspended in RNAlater (1 ml per 5 × 10⁶ cells). For systematic evaluation of different fixation protocols (Extended Data Fig. 1e–g), fixed cells had not been sorted but were either directly analysed upon fixation (30 min) or stored at –20 °C (ethanol-based fixatives) or 4 °C (others), respectively, overnight. To prepare RNAlater-fixed samples for sorting, tubes containing ~5 × 10⁶ fixed cells were filled up with 10 ml of ice-cold PBS, centrifuged (5 min, 500g, 4 °C) and cell pellets resuspended in 2 ml of cold PBS. This cell suspension was filtered and sorted (as described above).

RNA extraction, DNase treatment, evaluation of RNA quality and qRT-PCR. In the dual RNA-seq experiments, as a reference for gene expression changes in host cells upon infection, a non-infected yet mock-treated control was included. The bacterial reference samples were derived from *Salmonella* grown in LB to an OD₆₀₀ of 2.0, which either were then shifted to DMEM for 15 min, pelleted and fixed in RNAlater (see above) or were fixed directly (that is, without a medium exchange step) as indicated. Fixed *Salmonella* cells were pelleted and lysed using the lysis/binding buffer of the mirVana kit (Ambion). In order to maintain the approximate ratio of bacterial to host transcripts during RNA isolation, *Salmonella* lysates were mixed with host cell lysate in a way that the calculated proportion of individual *Salmonella* cells per infected host cell at the latest time point (see Extended Data Fig. 1h) was matched. The resulting mixture was then processed collectively. RNA was extracted from cells using the mirVana kit (Ambion) following the manufacturer's instructions for total RNA isolation. To remove contaminating genomic DNA, samples were treated with 0.25 U of DNase I (Fermentas) per 1 µg of RNA for 45 min at 37 °C. If applicable, RNA quality was checked on the Agilent 2100 Bioanalyzer (Agilent Technologies).

For qRT-PCR experiments total RNA was isolated using the TRIzol LS reagent (Invitrogen) according to the manufacturer's recommendations and treated with DNase I (Fermentas) as described above. qRT-PCR was performed with the Power SYBR Green RNA-to-CT 1-Step kit (Applied Biosystems) according to the manufacturer's instructions. Fold changes were determined using the 2^(-ΔΔCt) method⁶⁰. Primer sequences are given in Supplementary Table 1 and their specificity had been confirmed using Primer-BLAST (NCBI). For the estimation of *Salmonella* RNA within infection samples (Extended Data Fig. 1h), a dilution series of separately isolated *Salmonella* and HeLa-S3 total RNA was set up and in each case the ratio of *rfaH/ACTB* mRNAs was determined. The same was done for biological samples from infected cells as well as for the *Salmonella* reference controls. From the resulting trend-line equation the approximate proportion of the *Salmonella* transcriptome within mixed prokaryotic and eukaryotic total RNA samples could be deduced.

rRNA depletion (Ribo-Zero treatment). Where indicated (Supplementary Table 1), *Salmonella* and eukaryotic host rRNA were removed using the Ribo-Zero Magnetic Gold Kit (Epidemiology) purchased from Epicentre/Illumina. Following the manufacturer's instructions, ~500 ng of total, DNase-I-treated RNA from infection samples was used as an input to the ribosomal transcript removal procedure. rRNA-depleted RNA was precipitated in ethanol for 3 h at –20 °C.

cDNA library generation and (dual) RNA-seq. cDNA libraries for Illumina sequencing were generated by Vertis Biotechnologie AG, Freising-Weihenstephan, Germany. For dual RNA-seq of total RNA, at least 100 ng RNA were used for cDNA library preparation. DNase-I-treated total RNA samples were first sheared via ultra-sound sonication (4 pulses of 30 s at 4 °C each) to generate ~200–400 bp (average) fragmentation products. Fragments <20 nt were removed using the Agencourt RNAClean XP kit (Beckman Coulter Genomics). As an internal quality control for the pilot experiment (shown in Fig. 1), spike-in RNA (5'-AAAUCCGUUCGUACGGGCC-3'; 5'-monophosphorylated and

gel-purified) was added to a final concentration of 0.5%. The samples were poly(A)-tailed using poly(A) polymerase and the 5' triphosphate (or eukaryotic 5' cap) structures were removed using tobacco acid pyrophosphatase (TAP). Afterwards, an RNA adaptor was ligated to the 5' monophosphate of the RNA fragments. First-strand cDNA synthesis was performed using an oligo(dT)-adaptor primer and the M-MLV reverse transcriptase (NEB). The resulting cDNA was PCR-amplified to about 20–30 ng µl⁻¹ using a high fidelity DNA polymerase (barcode sequences for multiplexing were part of the 3' primers). The cDNA library was purified using the Agencourt AMPure XP kit (Beckman Coulter Genomics) and analysed by capillary electrophoresis (Shimadzu MultiNA microchip electrophoresis system).

cDNA libraries for dual RNA-seq on rRNA-depleted samples were constructed as described above, except for the following modifications. Upon RNA fragmentation, dephosphorylation with Antarctic Phosphatase (AP, NEB) and re-phosphorylation with T4 Polynucleotide Kinase (PNK, NEB) were performed. Oligonucleotide adaptors were ligated to both the 5' and 3' ends of the RNA samples. First-strand cDNA synthesis was performed using M-MLV reverse transcriptase and the 3' adaptor as primer.

cDNA libraries from *Salmonella*-only samples were generated by fragmenting 5 µg of total RNA using ultrasound and RNAs <20 nt were removed using the Agencourt RNAClean XP kit (Beckman Coulter Genomics) as above. The RNA samples were poly(A)-tailed and 5'pp structures were removed as before. RNA adaptors were ligated to the 5' monophosphate of the RNA and first-strand cDNA synthesis was performed using an oligo(dT)-adaptor primer and the M-MLV reverse transcriptase. The resulting cDNAs were PCR-amplified, purified using the Agencourt AMPure XP kit (Beckman Coulter Genomics) and analysed by capillary electrophoresis (Shimadzu MultiNA microchip).

Generally, for sequencing cDNA samples were pooled in approximately equimolar amounts. The cDNA pool was size-fractionated in the size range of 150–600 bp using a differential clean-up with the Agencourt AMPure kit. For the dual RNA-seq pilot experiment (Fig. 1), single-end sequencing (100 cycles) was performed on an Illumina HiSeq 2000 machine at the Max Planck Genome Centre Cologne, Cologne, Germany. For dual RNA-seq on rRNA-free samples as well as for conventional RNA-seq of *Salmonella*-only samples, single-end sequencing (75 cycles) was performed on a NextSeq500 platform at Vertis Biotechnologie AG, Freising-Weihenstephan, Germany.

All RNA-seq data discussed in this publication have been deposited in NCBI's Gene Expression Omnibus and are accessible through GEO Series accession number GSE60144. For the accession numbers of individual experiments, see Supplementary Table 1.

Northern blotting (of bacterial and human transcripts). Total RNA prepared with TRIzol LS reagent (Invitrogen) was separated in 6% (vol/vol) polyacrylamide-8.3 M urea gels and blotted as described¹¹. We loaded per lane either 5–10 µg of RNA from pure bacterial samples (Extended Data Figs 3d and 9a), 2 µg total RNA from sorted cell samples (Extended Data Fig. 8b), or 50 µg total RNA from unsorted infection samples (Fig. 2b). Hybond XL membranes (Amersham) were hybridized at 42 °C with gene-specific [³²P] end-labelled DNA oligonucleotides (see Supplementary Table 1 for sequences) in Hybri-Quick buffer (Carl Roth AG).

Mutational analysis of the *pinT* promoter region. The *pinT* promoter region was amplified by PCR using primers JVO-7036/-7037 and inserted via the *Aat*II and *Nhe*I sites in the backbone of plasmid pAS093, resulting in plasmid pYC65. To identify the PhoP binding sites in a minimal fragment, the *pinT* promoter region was truncated by amplifying pYC65 using Phusion polymerase (NEB) with JVO-9393/-7387. The critical residues in the PhoP binding motif (T_{–27}T_{–28}) were mutated to adenines by site-directed mutagenesis with JVO-12461/-12462 and Phusion polymerase (NEB).

sRNA pulse-expression (*in vitro* and *in vivo*). For pulse-expression of PinT in *in vitro* grown *Salmonella*, we used arabinose-induced overexpression of PinT from a pBAD plasmid previously described^{10,51,61} with minor modifications. Briefly, wild-type *Salmonella* that carried either a pKP8-35 (pBAD control), pYC5-34 (pBAD-PinT) or pYC60 (pBAD-PinT*) plasmid were grown overnight in LB and, the next day, the cultures were 1:100 diluted and further grown in LB to an OD₆₀₀ of 2.0. L-arabinose (Sigma) was added to a final concentration of 0.2%; 5 min later RNA was extracted using TRIzol LS reagent (Invitrogen) and analysed by RNA-seq (~3–5 million reads/library). For the same experiment under SPI-2-inducing conditions, overnight cultures of the three strains were washed 2× with PBS and 1× with SPI-2 medium²⁸, diluted 1:50 in SPI-2 medium and grown to an OD₆₀₀ of 0.3 before PinT expression was induced as above.

For the pulse-expression of PinT inside host cells (Extended Data Fig. 6d, e), HeLa-S3 cells were infected with the same three strains as above and 4 h after infection, 0.2% L-arabinose was supplemented directly into the DMEM medium. Activation of inducible sRNA expression in intracellular bacteria was confirmed by qRT-PCR over a time-course of 20 min (Extended Data Fig. 6d), demonstrating full induction levels to be reached already at 5 min. Thus, for Extended Data Fig. 6e

the host cells were lysed at 5 min after induction with ice-cold 0.1% Triton X-100/PBS and further incubated for 30 min on ice with pipetting up and down from time to time to improve host cell lysis efficiency. Then the intact bacterial cells were pelleted by centrifugation for 2 min at 16,100g (4 °C) and resuspended in RNAlater (Qiagen). The fixed bacterial cells were further enriched against the host background via cell sorting (FACSAria III, BD Biosciences) and selective gating for the fraction of GFP⁺ bacterial cells released from their hosts. From those, total RNA was isolated and analysed by RNA-seq as above except that sequencing was to a depth of ~20 million reads per library as necessitated by remaining host-derived RNA fragments.

Western blotting (of bacterial and human proteins). Immunoblotting of *Salmonella* proteins was done as previously described⁶². Briefly, samples from *Salmonella* *in vitro* cultures were taken corresponding to 0.4 OD₆₀₀, centrifuged for 4 min at 16,100g at 4 °C, and pellets resuspended in sample loading buffer to a final concentration of 0.01 OD per µl. After denaturation for 5 min at 95 °C, 0.05-OD equivalents of the sample were separated via SDS-PAGE. Gel-fractionated proteins were blotted for 90 min (0.2 mA per cm²; 4 °C) in a semi-dry blotter (Peplab) onto a PVDF membrane (Perkin Elmer) in transfer buffer (25 mM Tris base, 190 mM glycine, 20% methanol). Blocking was for 1 h at room temperature in 10% dry milk/TBST20. Appropriate primary antibodies (see Supplementary Table 1) were hybridized at 4 °C overnight and – following 3 × 10 min washing in TBST20 – secondary antibodies (Supplementary Table 1) for 1 h at room temperature.

For western blotting of human proteins, infected cells were harvested in sample loading buffer (500 µl per well; six-well format), transferred to 1.5 ml reaction tubes, boiled for 5 min at 95 °C and 20 µL per lane were loaded onto a 10% PAA gel for SDS-PAGE as above. After blotting and blocking (as above), the membrane was probed with the respective primary antibody at 4 °C overnight and – upon washing (as above) – with the secondary antibody for 1 h at room temperature (a full list with information about all antibodies and sera used is given in Supplementary Table 1).

After three additional washing steps for each 10 min in TBST20, blots were developed using western lightning solution (Perkin Elmer) in a Fuji LAS-4000. In Fig. 3e, intensities of protein bands were quantified using the AIDA software (Raytest, Germany) and normalized to GroEL levels.

In vitro SPI-1 to SPI-2 switch assay. To mimic the early stages of the infection of a host cell *in vitro*, the indicated *Salmonella* strains were grown in LB overnight, diluted 1:100 in LB and grown to an OD₆₀₀ of 2.0 (that is, a condition under which SPI-1 is highly induced^{4,11}), washed twice with PBS and once with SPI-2 medium²⁸ at room temperature, diluted 1:50 in pre-warmed SPI-2 medium (defined as t₀) and grown further in Erlenmeyer flasks at 37 °C for the indicated time periods. At the respective time points, samples were taken for RNA-seq, western blotting, and GFP fluorescence measurements.

Bacterial GFP reporter measurements (flow cytometry, plate reader). To measure the GFP intensity of reporter strains, bacteria were grown in LB in presence of Amp and Cm until an OD₆₀₀ of 2.0 was reached. *Salmonella* cells corresponding to 1 OD₆₀₀ were pelleted and fixed with 4% PFA. GFP fluorescence intensity was quantified for each 100,000 events by flow cytometry with the FACSCalibur instrument (BD Biosciences). Data were analysed using the Cyflogic software (CyFlo).

To monitor SPI-2 activation in real time, a transcriptional *gfp* reporter was constructed by inserting the SPI-2-dependent *ssaG* promoter into plasmid pAS0093 via *AatII/NheI* sites as previously described⁸. The resulting plasmid pYC104 was co-transformed with either the pBAD-ctrl. or pBAD-PinT plasmid into the indicated strain backgrounds. The resulting strains were grown overnight in LB (+Amp + Cm) and then diluted 1:100 and further grown in the same medium to an OD₆₀₀ of 2.0. A volume of 1 ml of the culture was pelleted and the collected cells shifted to SPI-2 medium²⁸ (defined as t₀) as described above, except that the growth experiment was conducted in 96-well plates (Nunc Microwell 96F, Thermo Scientific). After measuring the OD₆₀₀ and GFP intensity at t₀, L-arabinose was added to each well to final concentration of 0.2% for sRNA induction and bacteria were grown for 20 h at 37 °C (with shaking) with measurements of both the OD₅₉₅ and GFP fluorescence in 10 min intervals using the Infinite F200 PRO plate reader (Tecan).

Enzyme-linked immunosorbent assay (ELISA). HeLa-S3 cells were infected with wild-type *Salmonella*, ΔpinT or pinT+ mutant strains at an m.o.i. of 5 as described above. Culture supernatant samples were taken at 20 h p.i. and analysed using the ELISA kit for human CXCL8/IL-8 (R&D Systems).

Bioinformatic analyses. Code availability. In order to document the details and parameters of the (dual) RNA-seq data analyses and to make the biocomputational approaches reproducible for others, we implemented the workflows as Unix Shell scripts. These scripts are deposited at Zenodo (DOI: 10.5281/zenodo.34695, <https://zenodo.org/record/34695>). Please refer to Supplementary Table 1 for descriptions of the analyses.

Read processing and mapping. For all RNA-seq experiments listed in Supplementary Table 1, Illumina reads in FASTQ format were trimmed with a Phred quality score cut-off of 20 by the program fastq_quality_trimmer from FASTX toolkit version 0.0.13 (http://hannonlab.cshl.edu/fastx_toolkit/). Reads shorter than 20 nt after adaptor- and poly(A)-trimming were discarded before the mapping. The reads were aligned to the *Salmonella enterica* SL1344 genome (NCBI RefSeq accession numbers: NC_016810.1, NC_017718.1, NC_017719.1, NC_017720.1) and – where applicable – the human (hg19 – GRCh37; retrieved from the 1000 Genomes Project⁶³), the mouse (GENCODE M2, GRCm38.p2), or the porcine genome sequence (ENSEMBL, Sscrofa10.2), in parallel. The mapping was performed using the READemption pipeline (version 0.3.5)⁶⁴ and the short read mapper segemehl and its remapper lack (version 0.2.0)⁶⁵ allowing for split reads⁶⁶. Mapped reads with an alignment accuracy <90% as well as cross-mapped reads, that is, reads which could be aligned equally well to both host and *Salmonella* reference sequences, were discarded. The resulting data were used for visualization (see for example, Fig. 1b and Extended Data Fig. 2b).

Reads of the high resolution time-course experiment (cDNA libraries numbers 27–77 in Supplementary Table 1) that were detected as cross-mapped by READemption (see above) were further inspected: their median percentage over the entire time-course was 0.25% with increased fractions for the later time points, implying that those reads are mainly contributed by *Salmonella* cells. We observed that the majority of the cross-mapped reads aligned to *Salmonella* rRNA or tRNA loci, while on the human side no gene class preference was observed (data not shown).

Differential gene expression analysis. For dual RNA-seq experiments (cDNA libraries 1–184, 215–256 in Supplementary Table 1) after mapping differential expression analysis was carried out separately for the host and the pathogen. Strand-specific gene-wise quantifications for each data subset were performed by READemption⁶⁴. Host transcript expression analyses are based on annotations from GENCODE (version 19)⁶⁷, NONCODE (version 4)⁶⁸ and miRBase (version 20)⁶⁹ after removing redundant entries. The annotation for *Salmonella* genes was retrieved from NCBI (under the above mentioned accession numbers) and manually extended with small RNA annotations^{4,70}. In either organism, multi-mapped reads were removed and only uniquely mapped reads were considered for the expression analysis. Differential gene expression analyses were performed with the edgeR package (version 3.10.2)⁷¹ using an upper-quartile normalization and a prior count of 1. Where needed (that is, to correct for batch effects in the comparisons between wild-type and mutant infections; the comparisons displayed in Figs 3 and 4 and Extended Data Figs 5, 7–9), sequencing data were further normalized using the RUVs correction method⁷² with k = 3. For this purpose, we treated the samples time-point-wise to remove unwanted nuisance factors. At each time point our covariate of interest was the pinT status of the infecting bacterium. This is constant within replicate blocks, which are used for the RUVs correction. Host or bacterial genes with at least 10 uniquely mapped reads in three replicates were considered detected. Genes with an adjusted P value < 0.05 were considered differentially expressed. Differential expression analysis for conventional (bacteria only) RNA-seq experiments (cDNA libraries numbers 185–214 in Supplementary Table 1) was done similarly, except that a cut-off of ≥50 uniquely mapped reads was used as a detection threshold.

Read coverage plots. Based on the obtained BAM files, coverage files in wiggle format were generated by READemption⁶⁴ in a strand-specific manner and split by organism. In each case, coverage files are based on uniquely mapped reads and normalized by the total number of uniquely aligned reads per organism. For Fig. 4e, wiggle files were visualized using the Integrated Genome Browser (version 8.4.4)⁷³.

Pathway enrichment and further analyses for *Salmonella*. A database of pathways, regulons, and genomic islands was constructed using information obtained from the KEGG database⁷⁴ (organism code sey), the SL1344 genome annotation⁷⁰, and relevant literature sources (see Supplementary Table 1). Pearson correlation coefficients between changes in PinT expression and changes in expression of each gene within each regulon over the time-course of wild-type *Salmonella* infection (cDNA libraries number 27, 30, 33, 36, 39, 42, 44, 47, 50, 53, 56, 59, 61, 64, 67, 70, 73, 76 in Supplementary Table 1) were plotted in Fig. 2d.

To assess enrichment of differentially expressed transcripts in pathways in the comparative infection experiments (cDNA libraries numbers 27–77 and 152–184 in Supplementary Table 1) and the *in vitro* assay (cDNA libraries numbers 185–202 in Supplementary Table 1), gene set enrichment analysis (GSEA; version 2.1.0) was run on the log₂ fold changes reported by edgeR. The GSEA was performed in ranked list mode (with statistic classic) and gene sets containing less than 15 or more than 100 entries were excluded. Extended Data Fig. 5a reports all pathways significant at an FDR-corrected P value of at most 0.05 in at least one time point.

Host pathway analysis and inspection of alternative isoform expression. Host pathway enrichment studies were performed consistently with bacterial analyses using GSEA on human pathways available in the KEGG database (downloaded

January 22, 2014) using the same settings described above. Pathways with an adjusted P value ≤ 0.05 were considered to be significantly modulated. Data visualization for Extended Data Fig. 8a was produced using the Bioconductor package Pathview⁷⁵. Genes displayed in Fig. 1d, that is, genes whose transcription is known or predicted to be regulated by the binding of nuclear factor κ B (NF- κ B) to their promoter or genes whose products have been shown to promote an NF- κ B response, were retrieved from the GeneCards⁷⁶ and Boston University Biology (<http://www.bu.edu/nf-kb/gene-resources/target-gene>) databases or refs 77, 78. STAT3 target genes denoted in Fig. 4b were retrieved from ref. 79.

We used Cufflinks/Cuffdiff (version 2.2.1)^{80,81} to test for differentially expressed isoforms in the high-resolution, comparative dual RNA-seq time-course data set (cDNA libraries number 27–77 in Supplementary Table 1). In a first step, we used Cufflinks to quantify transcript isoforms in the mapped read data. Afterwards, all transcript annotations were merged using Cuffmerge and differentially expressed isoforms were called using Cuffdiff.

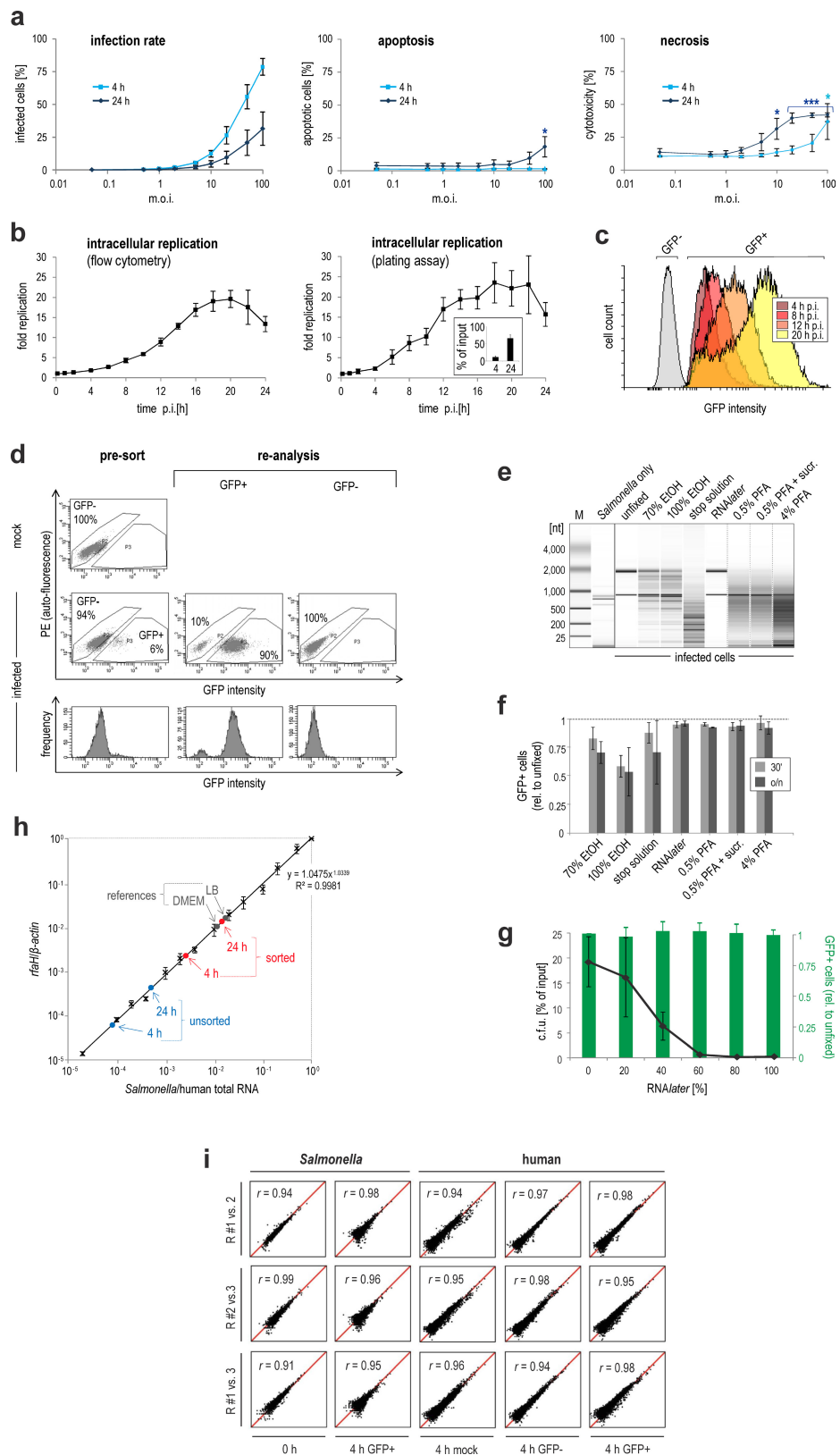
Interspecies correlation analysis of pathogen and host transcriptome changes. To identify bacterial and human genes with similar expression kinetics across the time-course of the infection of HeLa-S3 cells (cDNA libraries number 27–77 in Supplementary Table 1), we used RUVs-corrected, abundance-filtered and normalized read counts (see above). Absolute counts were then transformed into standard z-scores for each gene over all considered samples as follows: for each gene, the z-score was calculated as the absolute read count minus the mean read count over all samples, divided by the standard deviation of all counts over all samples. Genes with a standard deviation <2 were excluded from further analysis. Pearson correlation coefficients were calculated between all remaining bacterial genes and all remaining human genes, and P values were calculated using the function cor.test in R. To account for a possible temporal delay between *Salmonella* expression changes and effect manifestation in the host cell, a time-shift was allowed. This means the expression of *Salmonella* genes at each time point was compared to host expression at the subsequent time point. Human genes were considered to be correlated with a bacterial gene if they had a P value of less than 10^{-4} and a Pearson's r greater than 0.65. This resulted in a total of 751 clusters of human genes showing correlation in expression with a bacterial gene, approximately half of which (see Supplementary Table 1) had at least one enriched GO term associated with them (adjusted P value < 0.05) as tested using the software tool Ontologizer 2.0 (build: 20100310-351)⁸² with the gene ontology definition obtained from the Gene Ontology Consortium (data-version: releases/2015-09-26) and the Universal Protein Resource (UniProt) gene annotation (generated: 2015-09-14).

To account for the possibility that multiple bacterial genes might be associated with a human gene cluster a correlation analysis was performed for all against all bacterial genes as described above, with the only exception that no time-shift was allowed. For this, we focused on seventeen gene clusters that were built on bacterial genes encoding for secretion-associated gene products (according to UniProt; see Supplementary Table 1). Detailed inspection of these clusters revealed the one depicted in Fig. 4b (centred on the bacterial SPI-2 gene *sseC*) which contained many further (bacterial and human) genes with pronounced PinT-dependent expression changes – that is, genes that showed differential expression between wild-type and Δ pinT infection at several time points p.i.

Statistics. In all RNA-seq-based analyses, transcript expression changes that were associated with an adjusted P value < 0.05 (reported by edgeR) were considered significantly differentially expressed. For Fig. 3b, a Monte Carlo permutation test was performed on the median fold change of genes in the SPI-2 regulon, using 10^5 randomly selected gene sets of the same size. This indicated the significant de-repression ($P < 0.05$) of the SPI-2 regulon in the absence of PinT at 2 and 8 h after the infection of HeLa cells, at 2, 6 and 16 h after the infection of 3D4/31 cells, and in the *in vitro* assay. Tests for the evaluation of increased host cell death in Extended Data Fig. 1a were performed using a one-tailed Student's t -test. * P values ≤ 0.05 were considered significant and *** P values ≤ 0.001 were considered very significant. The significance of gene activation in qRT-PCR results in Fig. 4c and Extended Data Figs 5b, c and 7c, d or the ELISA assay in Extended Data Fig. 7e was assessed using a one-tailed Mann-Whitney U -test. The significance of differences in intracellular replication between the Δ pinT strain and wild-type *Salmonella* (Extended Data Fig. 4d) was evaluated using a two-tailed Mann-Whitney U -test.

51. Papenfort, K. et al. Specific and pleiotropic patterns of mRNA regulation by ArcZ, a conserved, Hfq-dependent small RNA. *Mol. Microbiol.* **74**, 139–158 (2009).
52. Datsenko, K. A. & Wanner, B. L. One-step inactivation of chromosomal genes in *Escherichia coli* K-12 using PCR products. *Proc. Natl. Acad. Sci. USA* **97**, 6640–6645 (2000).
53. Sternberg, N. L. & Maurer, R. Bacteriophage-mediated generalized transduction in *Escherichia coli* and *Salmonella typhimurium*. *Methods Enzymol.* **204**, 18–43 (1991).

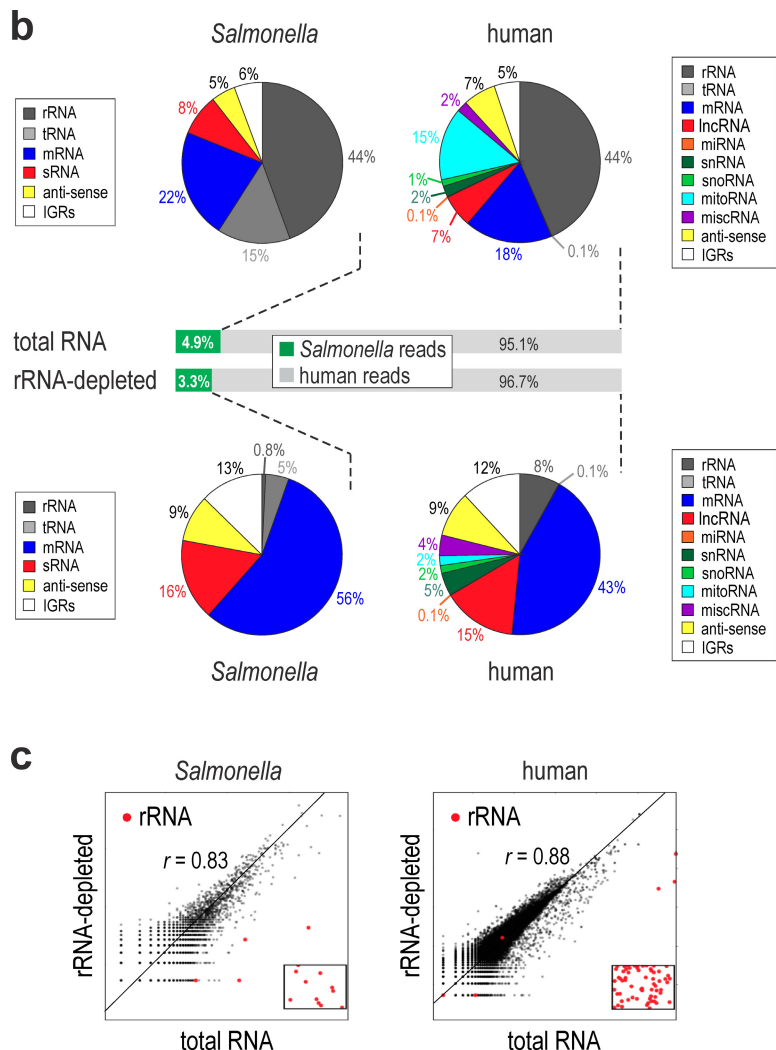
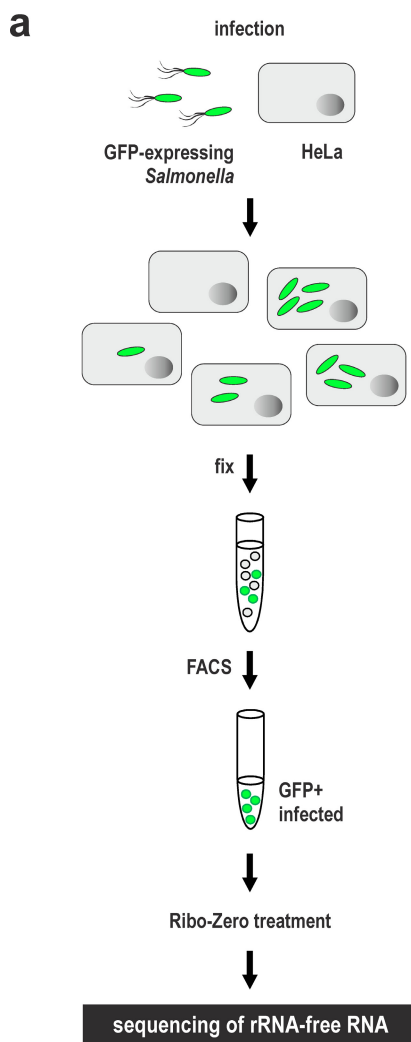
54. Berschneider, H. M. Development of normal cultured small intestinal epithelial cell lines which transport Na and Cl. *Gastroenterology* **96**:A41 (1989).
55. Weingartl, H. M., Sabara, M., Pasick, J., van Moorhem, E. & Babiuk, L. Continuous porcine cell lines developed from alveolar macrophages: partial characterization and virus susceptibility. *J. Virol. Methods* **104**, 203–216 (2002).
56. Schulte, L. N., Eulalio, A., Mollenkopf, H. J., Reinhardt, R. & Vogel, J. Analysis of the host microRNA response to *Salmonella* uncovers the control of major cytokines by the let-7 family. *EMBO J.* **30**, 1977–1989 (2011).
57. Eriksson, S., Lucchini, S., Thompson, A., Rhen, M. & Hinton, J. C. Unravelling the biology of macrophage infection by gene expression profiling of intracellular *Salmonella enterica*. *Mol. Microbiol.* **47**, 103–118 (2003).
58. Hamatani, K. et al. Improved RT-PCR amplification for molecular analyses with long-term preserved formalin-fixed, paraffin-embedded tissue specimens. *J. Histochem. Cytochem.* **54**, 773–780 (2006).
59. Kuramochi, H. et al. Vascular endothelial growth factor messenger RNA expression level is preserved in liver metastases compared with corresponding primary colorectal cancer. *Clin. Cancer Res.* **12**, 29–33 (2006).
60. Livak, K. J. & Schmittgen, T. D. Analysis of relative gene expression data using real-time quantitative PCR and the $2^{-\Delta\Delta CT}$ Method. *Methods* **25**, 402–408 (2001).
61. Papenfort, K. et al. σ^E -dependent small RNAs of *Salmonella* respond to membrane stress by accelerating global *omp* mRNA decay. *Mol. Microbiol.* **62**, 1674–1688 (2006).
62. Urban, J. H. & Vogel, J. Translational control and target recognition by *Escherichia coli* small RNAs in vivo. *Nucleic Acids Res.* **35**, 1018–1037 (2007).
63. The 1000 Genomes Project Consortium An integrated map of genetic variation from 1,092 human genomes. *Nature* **491**, 56–65 (2012).
64. Förstner, K. U., Vogel, J. & Sharma, C. M. READemption—a tool for the computational analysis of deep-sequencing-based transcriptome data. *Bioinformatics* **30**, 3421–3423 (2014).
65. Otto, C., Stadler, P. F. & Hoffmann, S. Lacking alignments? The next-generation sequencing mapper segemehl revisited. *Bioinformatics* **30**, 1837–1843 (2014).
66. Hoffmann, S. et al. A multi-split mapping algorithm for circular RNA, splicing, trans-splicing, and fusion detection. *Genome Biol.* **15**, R34 (2014).
67. Harrow, J. et al. GENCODE: the reference human genome annotation for The ENCODE Project. *Genome Res.* **22**, 1760–1774 (2012).
68. Xie, C. et al. NONCODEv4: exploring the world of long non-coding RNA genes. *Nucleic Acids Res.* **42**, D98–D103 (2014).
69. Kozomara, A. & Griffiths-Jones, S. miRBase: annotating high confidence microRNAs using deep sequencing data. *Nucleic Acids Res.* **42**, D68–D73 (2014).
70. Kroger, C. et al. The transcriptional landscape and small RNAs of *Salmonella enterica* serovar Typhimurium. *Proc. Natl. Acad. Sci. USA* **109**, E1277–E1286 (2012).
71. Robinson, M. D., McCarthy, D. J. & Smyth, G. K. edgeR: a Bioconductor package for differential expression analysis of digital gene expression data. *Bioinformatics* **26**, 139–140 (2010).
72. Risso, D., Ngai, J., Speed, T. P. & Dudoit, S. Normalization of RNA-seq data using factor analysis of control genes or samples. *Nature Biotechnol.* **32**, 896–902 (2014).
73. Nicol, J. W., Helt, G. A., Blanchard, S. G., Raja, A. & Loraine, A. E. The Integrated Genome Browser: free software for distribution and exploration of genome-scale datasets. *Bioinformatics* **25**, 2730–2731 (2009).
74. Kanehisa, M. et al. Data, information, knowledge and principle: back to metabolism in KEGG. *Nucleic Acids Res.* **42**, D199–D205 (2014).
75. Luo, W. & Brouwer, C. Pathview: an R/Bioconductor package for pathway-based data integration and visualization. *Bioinformatics* **29**, 1830–1831 (2013).
76. Rebhan, M., Chalifa-Caspi, V., Prilusky, J. & Lancet, D. GeneCards: integrating information about genes, proteins and diseases. *Trends Genet.* **13**, 163 (1997).
77. Choi, Y. S. et al. Nuclear IL-33 is a transcriptional regulator of NF- κ B p65 and induces endothelial cell activation. *Biochem. Biophys. Res. Commun.* **421**, 305–311 (2012).
78. Oida, Y. et al. Inhibition of nuclear factor- κ B augments antitumor activity of adenovirus-mediated melanoma differentiation-associated gene-7 against lung cancer cells via mitogen-activated protein kinase kinase kinase 1 activation. *Mol. Cancer Ther.* **6**, 1440–1449 (2007).
79. Dauer, D. J. et al. Stat3 regulates genes common to both wound healing and cancer. *Oncogene* **24**, 3397–3408 (2005).
80. Trapnell, C. et al. Transcript assembly and quantification by RNA-Seq reveals unannotated transcripts and isoform switching during cell differentiation. *Nature Biotechnol.* **28**, 511–515 (2010).
81. Trapnell, C. et al. Differential analysis of gene regulation at transcript resolution with RNA-seq. *Nature Biotechnol.* **31**, 46–53 (2013).
82. Bauer, S., Grossmann, S., Vingron, M. & Robinson, P. N. Ontologizer 2.0—a multifunctional tool for GO term enrichment analysis and data exploration. *Bioinformatics* **24**, 1650–1651 (2008).
83. Soncini, F. C., Vescovi, E. G. & Groisman, E. A. Transcriptional autoregulation of the *Salmonella typhimurium phoPQ* operon. *J. Bacteriol.* **177**, 4364–4371 (1995).
84. Rehmsmeier, M., Steffen, P., Hochsmann, M. & Giegerich, R. Fast and effective prediction of microRNA/target duplexes. *RNA* **10**, 1507–1517 (2004).



Extended Data Figure 1 | See next page for caption.

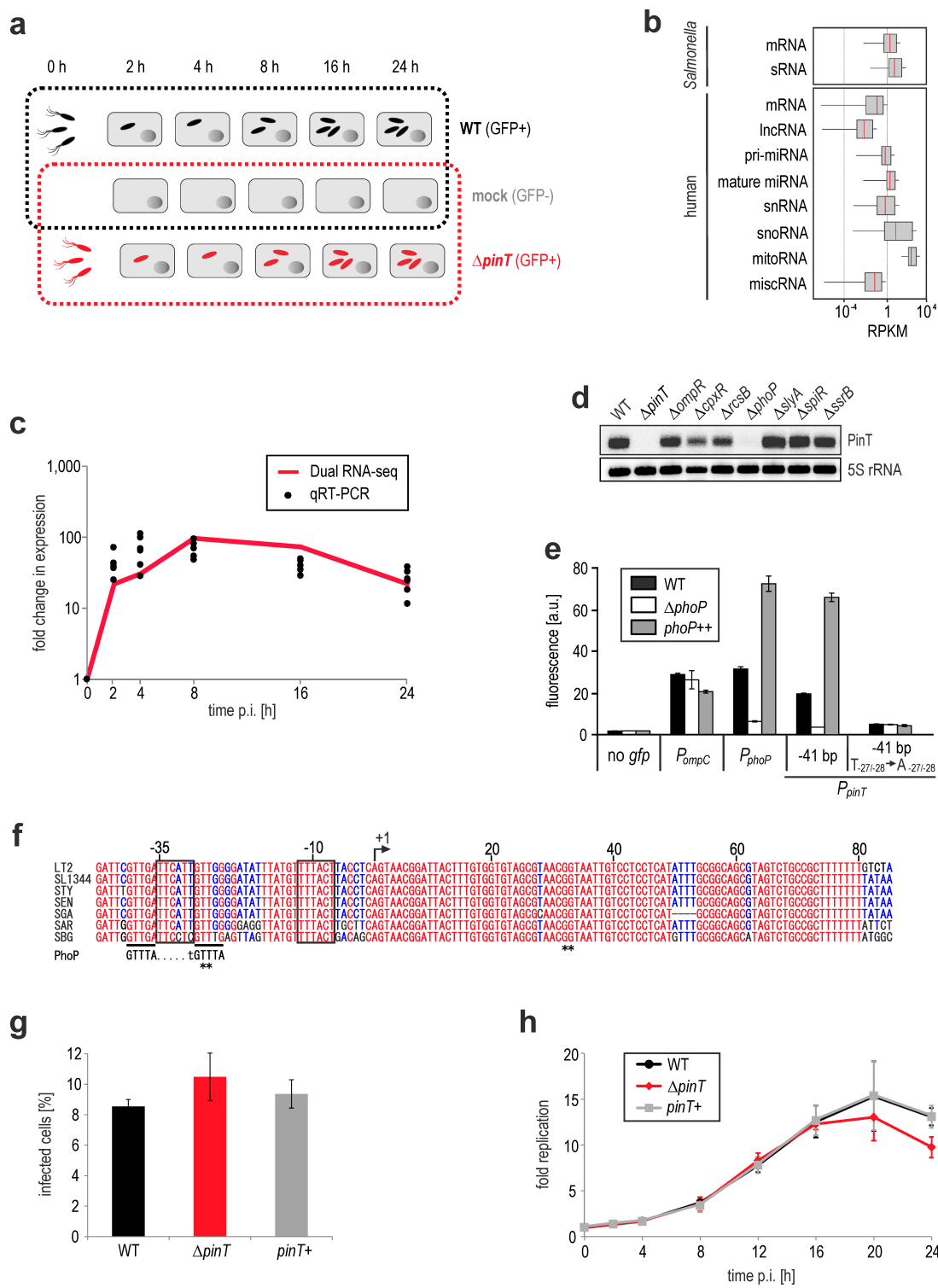
Extended Data Figure 1 | Establishment of the infection model with HeLa-S3 cells and constitutively GFP-expressing *Salmonella*. **a**, Rate of infected, apoptotic and cytotoxic HeLa-S3 cells over a range of different m.o.i.s. Left panel: infectivity increases with increasing bacterial doses. The discrepancy between the fractions of infected cells at 4 h and 24 h p.i. results from increasing levels of host cell death over time. Quantification of infectivity was achieved via flow cytometry (FACSCalibur, BD Biosciences) and the Cyflogic software (CyFlo) by gating for the GFP⁺ and GFP⁻ populations. Middle: apoptosis measurement by annexin V-APC (BD Pharmingen)/propidium iodide (PI) (Sigma) staining followed by flow cytometry using the MACSQuant Analyzer device (Miltenyi Biotec). APC-positive/PI-negative cells were considered apoptotic. Right: lactate dehydrogenase (LDH) release as a proxy for necrosis in infected HeLa-S3 cultures. The colorimetric product was quantified by measuring the absorbance at 490 nm. 100% host cell death was determined by treating the cell culture with lysis buffer before analysis. * $P \leq 0.05$; *** $P \leq 0.001$ (one-tailed Student's *t*-test). **b**, Intracellular replication of *Salmonella* inside HeLa-S3 (m.o.i. of 5). Left panel, flow cytometry-based quantification of the increase in GFP intensity per infected host cell over time (see also panel c and Methods). Right: c.f.u. counts. The inset illustrates the relative amount of intracellular bacteria at 4 or 24 h p.i., respectively, as compared to the input. Combination of infectivity (panel a) and c.f.u. data (panel b) allows for the calculation of the average number of intracellular bacteria per invaded cell at distinct time points: 4 h p.i.: ~10 bacteria; 24 h p.i.: ~75 bacteria. **c**, Representative overlay histogram of flow cytometry data exemplifying the increase in GFP intensity per infected HeLa-S3 cell over time. Plot was generated using the Flowing software (Turku Centre for Biotechnology, Finland). **d**, Representative FACS plots showing the

gating strategy for the separation of invaded and non-invaded HeLa-S3 cells. The signal detected in the phycoerythrin (PE) channel was used as a proxy for a cell's autofluorescence. The percentage values indicate the relative proportion of GFP⁺ and GFP⁻ cells before ('pre-sort') and after sorting ('re-analysis'). **e**, Capillary electrophoresis of total RNA samples from infected cells (4 h p.i.) that were fixed overnight using different reagents. Stop solution refers to 95% EtOH/5% phenol. Where indicated ('+sucr') paraformaldehyde (PFA) was supplemented with 2% sucrose. The band pattern of pure *Salmonella* RNA is shown to the left. Note that in the infection samples bacterial rRNA bands are not visible due to the overwhelming host RNA background. For gel source data, see Supplementary Fig. 1. **f**, Influence of different preservatives on FACS-based recovery of invaded host cells through bleaching of the GFP signal. **g**, Increasing concentrations of RNAlater kill intracellular *Salmonella* (black line) but do not compromise detection of GFP fluorescence (green bars). **h**, Extrapolation of the relative representation of *Salmonella* and human transcriptomes in infection samples. A dilution series of separately isolated *Salmonella* to HeLa-S3 total RNA was set up and for each ratio, bacterial *rfaH* (relative to human *ACTB*) mRNA was quantified by qRT-PCR. The resulting trend-line equation was used to infer the percentage of the *Salmonella* transcriptome within mixed total RNA samples from infected HeLa-S3 cells at different time points and without (blue) or upon FACS-based enrichment for invaded cells (red). The position of medium control samples (LB, DMEM) is given in grey. **i**, Normalized read counts for all detected *Salmonella* or human genes at 4 h p.i. are plotted for 3 biological replicate experiments and the Pearson correlation coefficient (*r*) is given. Panels a, b, f, g, h show the mean ± s.d. from each 3 biological replicates.



Extended Data Figure 2 | Establishment of an rRNA-depletion step for dual RNA-seq. **a**, Experimental workflow. **b**, Comparative mapping statistics of dual RNA-seq samples without (upper panel) or upon the joint depletion of bacterial and eukaryotic rRNA using the Ribo-Zero Gold (Epidemiology) kit (lower panel). **c**, Gene-wise correlation between read

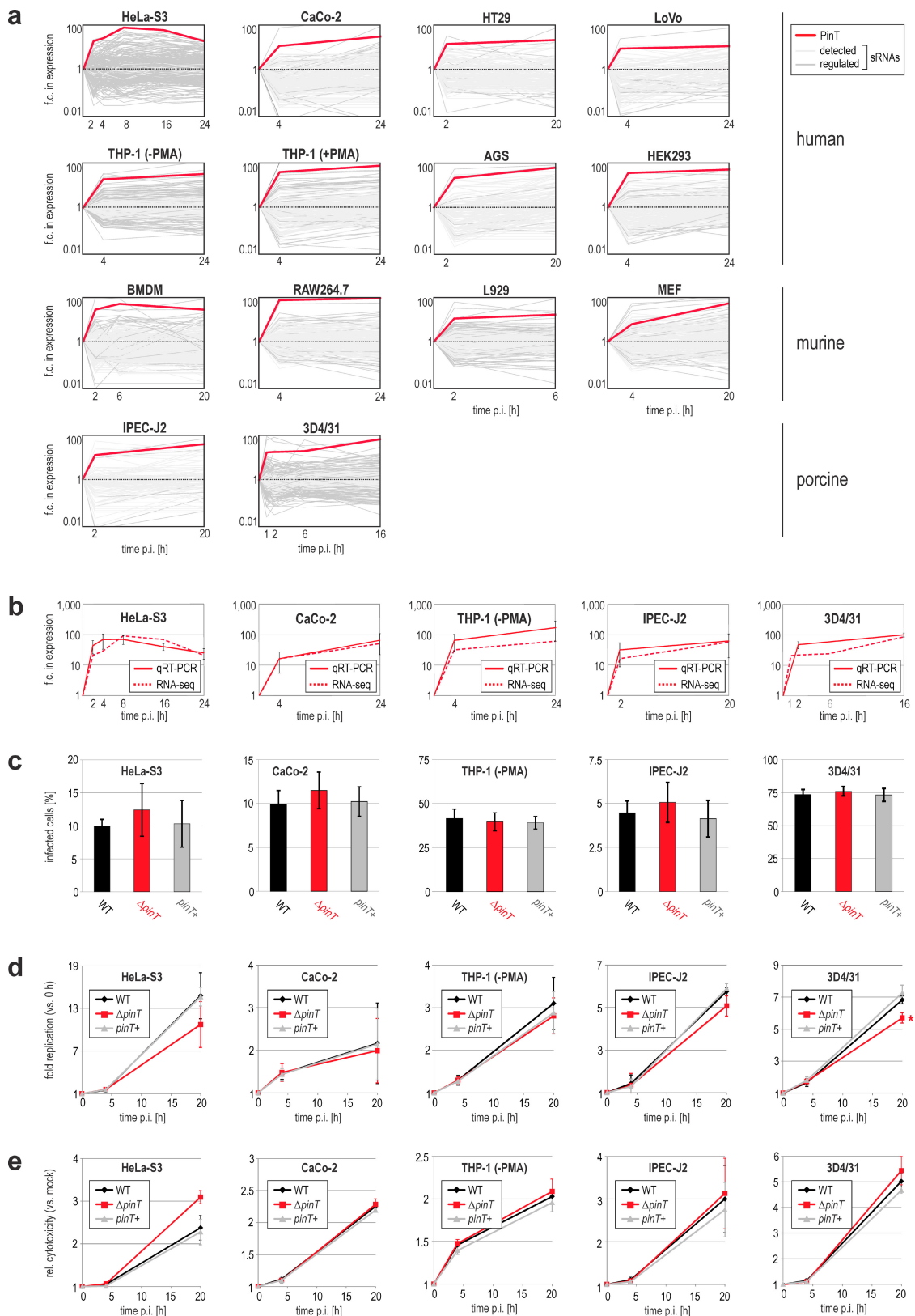
coverages without or upon rRNA removal for *Salmonella* (left) and human (right) data subsets. The Pearson's r is given. The red dots in squares represent the rRNA transcripts that had zero reads in the rRNA-depleted sample.



Extended Data Figure 3 | See next page for caption.

Extended Data Figure 3 | PinT is induced during infection via PhoP binding to its promoter region. **a**, Scheme of the comparative high-resolution time-course analysed by dual RNA-seq. For both the *Salmonella* strains, five individual time points post-invasion of HeLa-S3 cells were sampled and enriched for the fraction of invaded (GFP^+) host cells. Mock-treated cells were used as a host, and extracellular *Salmonella* in DMEM medium (0 h) as a bacterial reference control. Together this resulted in 17 different conditions which were sampled as biological triplicates. **b**, Average RPKM distribution over individual *Salmonella* or human transcript classes from the wild-type infection time-course. **c**, PinT activation during invasion of HeLa-S3 cells as revealed by dual RNA-seq (red graph) can be reproduced by qRT-PCR measurements (black dots; each dot represents a single out of 4 (2; 8; 16 h), 5 (4 h) or 6 biological replicate experiments (24 h)). Normalization was achieved using the constitutively expressed *gfp* mRNA as a reference. **d**, Northern blot detection of PinT in the *Salmonella* wild-type and various mutant backgrounds in which the indicated global regulators were deleted. For gel source data, see Supplementary Fig. 1. **e**, Mutational analysis identifies PhoP as a direct transcriptional activator of the *pinT* promoter. A transcriptional *gfp* fusion construct containing the *pinT* upstream promoter region (-41 bp to +5 bp) was analysed in the wild-type,

phoP deletion or *phoP* complementation backgrounds. A non-fluorescent ('no *gfp*') or unrelated *ompC* promoter reporter served as negative controls and a *phoP* promoter reporter as a positive control (as PhoP is known to auto-regulate its own expression⁸³). Two-nucleotide exchanges ($T_{-271-28} \rightarrow A_{-271-28}$) in the predicted PhoP binding site (see alignment in panel f) are sufficient to abrogate PhoP responsiveness of PinT expression. Error bars indicate the s.d. from the mean from biological triplicates. **f**, Sequence alignment shows the conservation of PinT sRNA within the genus *Salmonella*. "STY": *S. Typhi*, "SEN": *S. Enteritidis*, "SGA": *S. Gallinarum*, "SAR": *S. arizona*, "SBG": *S. bongori*. Perfectly conserved ribonucleobases are labelled in red, less conserved bases are shown in blue. The numbers indicate the position relative to the 5' end of PinT (+1 position). Black lines and sequence motif below the alignment highlight a PhoP binding site (the asterisks denote thymines that were converted into adenines for mutational analysis in panel e). Asterisks below the seed sequence (position ~30–40) mark two guanines that were mutated to cytosines in Fig. 3 and Extended Data Fig. 6. **g, h**, Infection rate (g) and intracellular replication kinetics (h) of the indicated *Salmonella* strains in HeLa-S3 cells (m.o.i. of 5). Data are derived from flow cytometry measurements as described for Extended Data Fig. 1a, b, and refer to the mean \pm s.d. from 3 biological replicates.

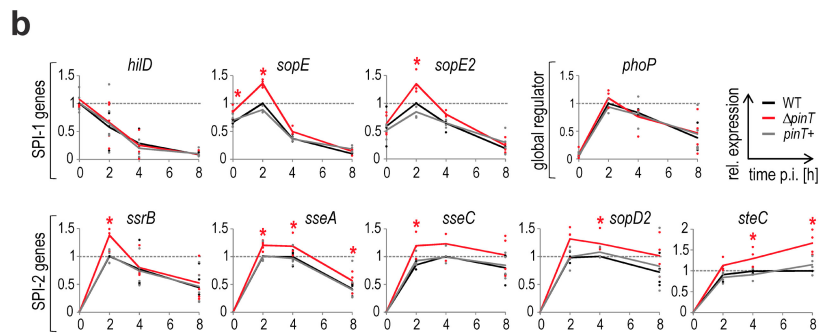
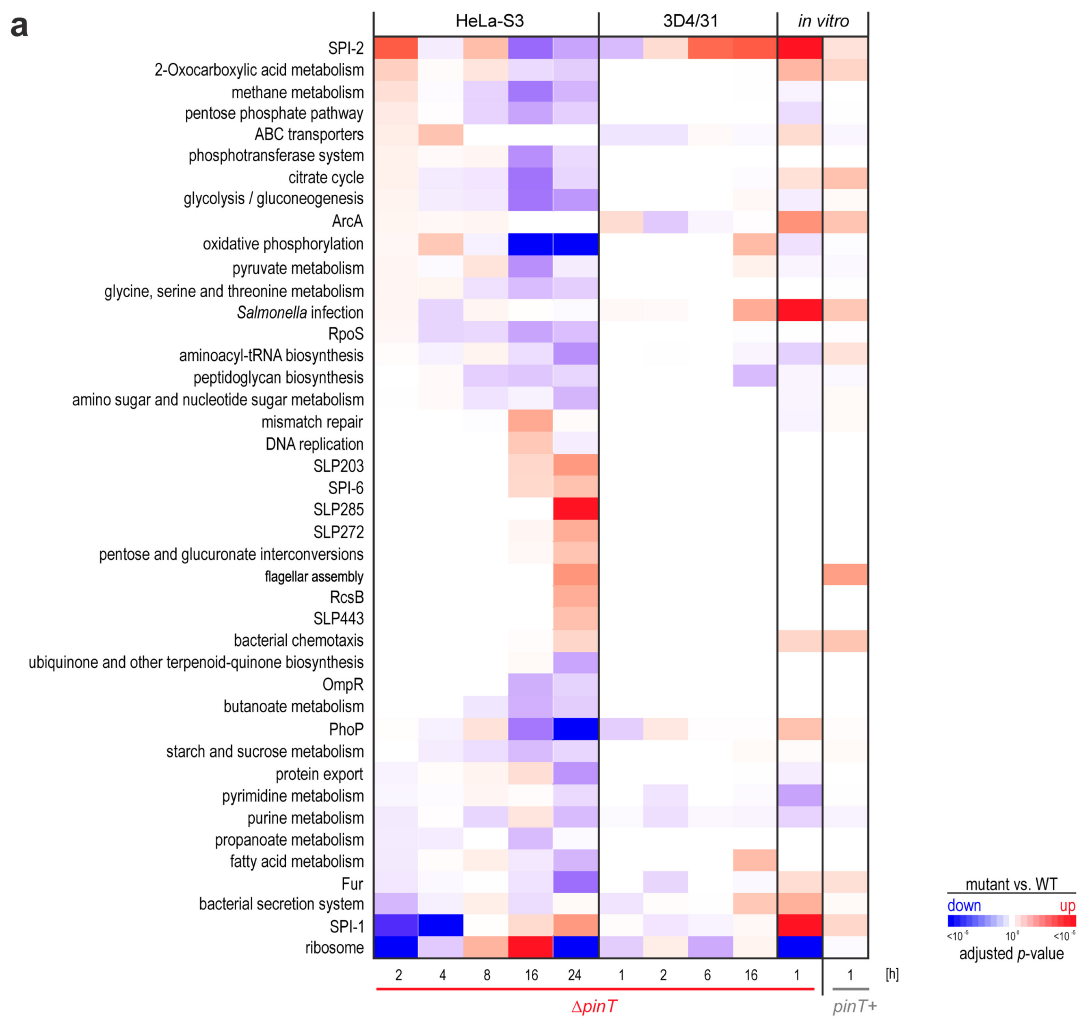


Extended Data Figure 4 | See next page for caption.

Extended Data Figure 4 | PinT is strongly induced upon the invasion of diverse host cell types while its deletion only has slight effects in cell culture models. **a**, The given cell types were infected with wild-type *Salmonella* for the indicated time periods and total or rRNA-depleted RNA (as indicated in Supplementary Table 1) was sequenced. THP-1 cells either were differentiated by treating them with phorbol myristate acetate before infection ('+PMA') or were kept monocytic ('-PMA'). For all but HeLa-S3 cells and porcine cell types infection was established at an m.o.i. of 10. IPEC-J2 and 3D4/31 cells were infected at an m.o.i. of 20 and HeLa-S3 at an m.o.i. of 5. Shown are detected (≥ 10 reads in each replicate; light grey) and regulated sRNAs (adjusted P value < 0.05 ; dark grey). The data was derived from 3 biological replicates for HeLa-S3 and 3D4/31 and 2 biological replicates for the other cell types. PinT expression (red line) was significantly upregulated in all cell types. **b**, qRT-PCR validation of the induction of PinT in five selected host cell types. qRT-PCR data from 3 biological replicates were drawn (solid lines). Normalization was against *gfp* mRNA. The data from HeLa-S3 is the same as in Extended Data Fig. 3c.

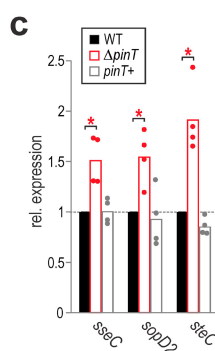
For comparison, in each case the RNA-seq-based expression data of PinT (as shown in panel **a**) are re-plotted (dashed curves).

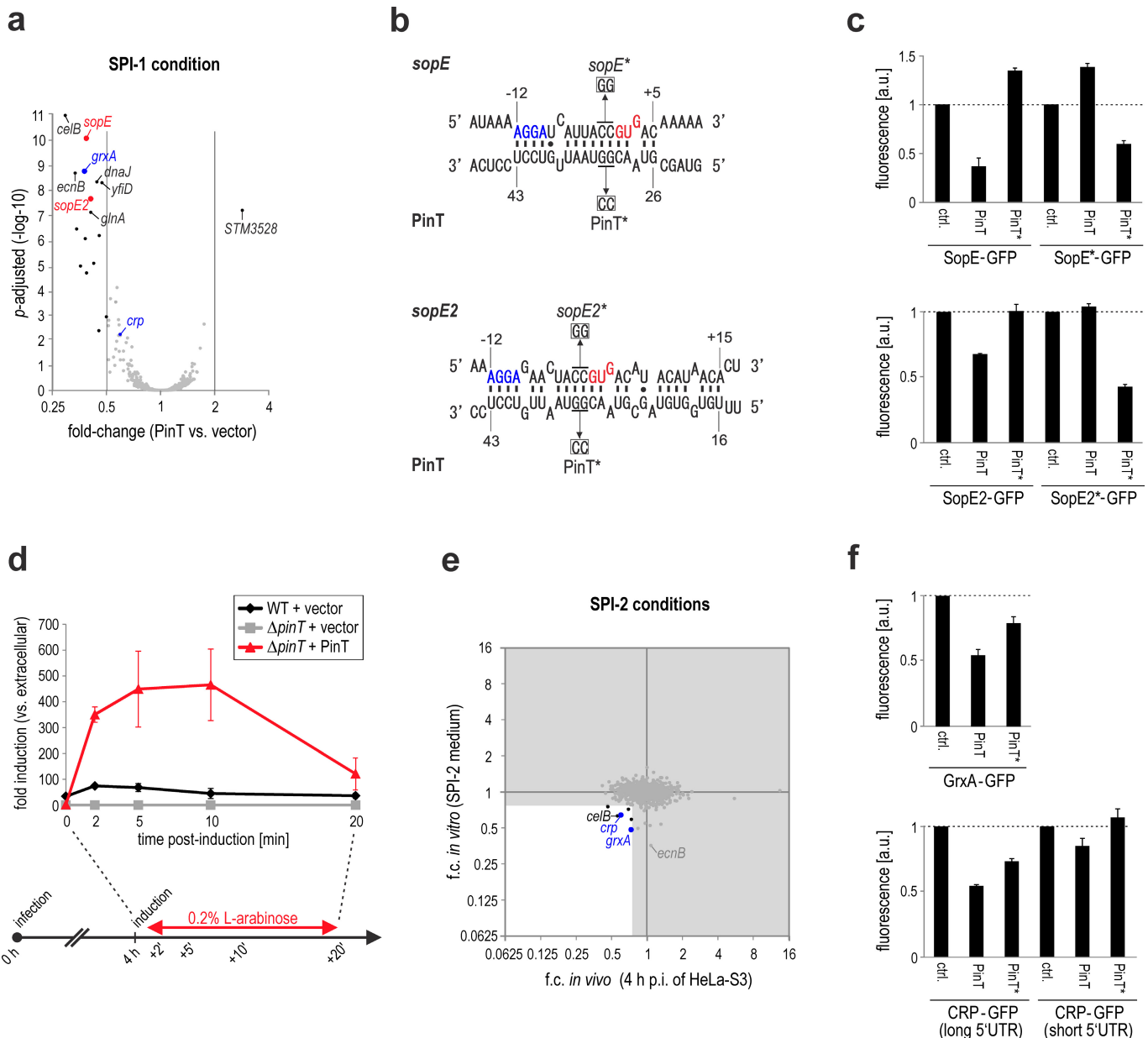
c, Invasion assays for wild-type, ΔpinT and *pinT*⁺ *Salmonella* with HeLa-S3 (m.o.i. 5), CaCo-2 and undifferentiated THP-1 (both m.o.i. 10), as well as IPEC-J2 and 3D4/31 (both m.o.i. 20). In all cases, the invasion rate was profiled 10 min p.i. by flow cytometry. **d**, Intracellular replication kinetics for the same strains and host cell types. The increase in GFP intensity of infected cells over time was monitored by flow cytometry and expressed as fold change compared to the t_0 time point (see Methods). The asterisk denotes a significantly different replication rate between the wild-type and ΔpinT strain ($P < 0.05$; two-tailed Mann–Whitney U -test). **e**, Host cell cytotoxicity measurements for the same host cell types upon infection with the indicated *Salmonella* strains. At the respective time points p.i., LDH activity in the supernatant of the infected cultures was quantified and the increase over time was with respect to the LDH activity measured in supernatants of mock-infected cells. The data in panels **c–e** represent the mean \pm s.d. from 3 biological replicates.



Extended Data Figure 5 | *Salmonella* PinT sRNA represses SPI-2 expression during the infection of HeLa-S3 cells and pig macrophages.
a, The heat map shows the result from gene set enrichment analyses of *Salmonella* gene expression data from the comparative dual RNA-seq time-course experiments with HeLa-S3 cells and porcine 3D4/31 macrophages, and from the comparative RNA-seq experiment of *Salmonella* grown for 1 h under SPI-2-inducing *in vitro* conditions. It reveals the de-repression of SPI-2 genes in the absence of PinT (ΔpinT) at several time points—a specific effect as SPI-2 expression reverts to wild-type levels upon *trans*-complementation of PinT (pinT^+) in the *in vitro* assay. **b**, qRT-PCR measurements during the early stages of HeLa-S3

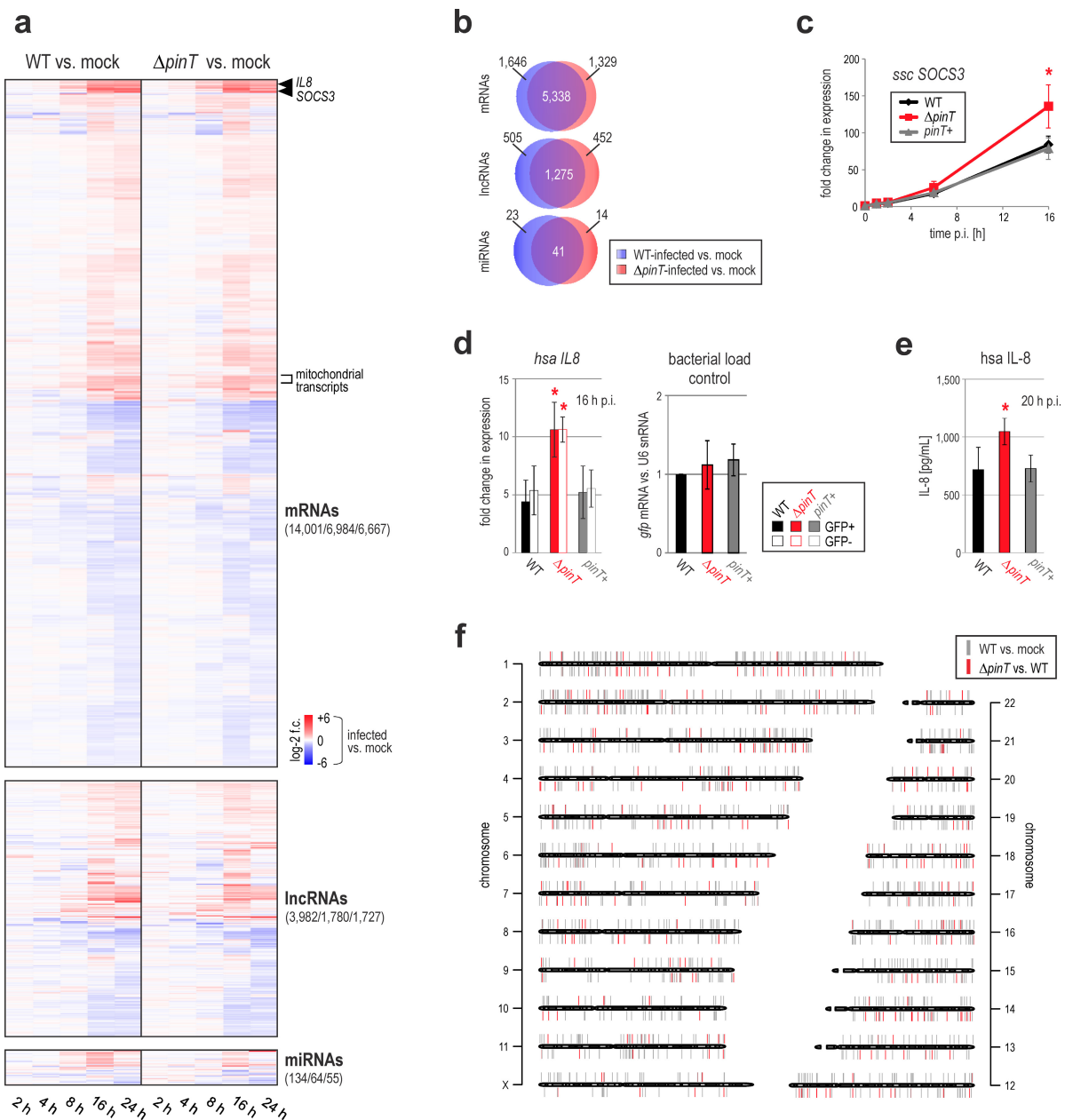
infection validates the de-repression of *Salmonella* SPI-2 genes in the ΔpinT background (red) as compared to both wild-type (black) and pinT^+ (grey) strains. Normalization was performed using *gfp* mRNA. Dots represent individual biological replicate experiments (five for *hilD*, *sseA*, *ssrB*; four for the other mRNAs) and the solid lines indicate their mean. **c**, qRT-PCR validation of de-repressed SPI-2 genes 6 h after the invasion of pig macrophages. Porcine GAPDH mRNA was used for normalization. The data represent the results from biological triplicate measurements. The asterisks in panels **b** and **c** denote significantly increased transcript levels in ΔpinT compared to wild-type *Salmonella* ($P < 0.05$; one-tailed Mann–Whitney *U*-test).





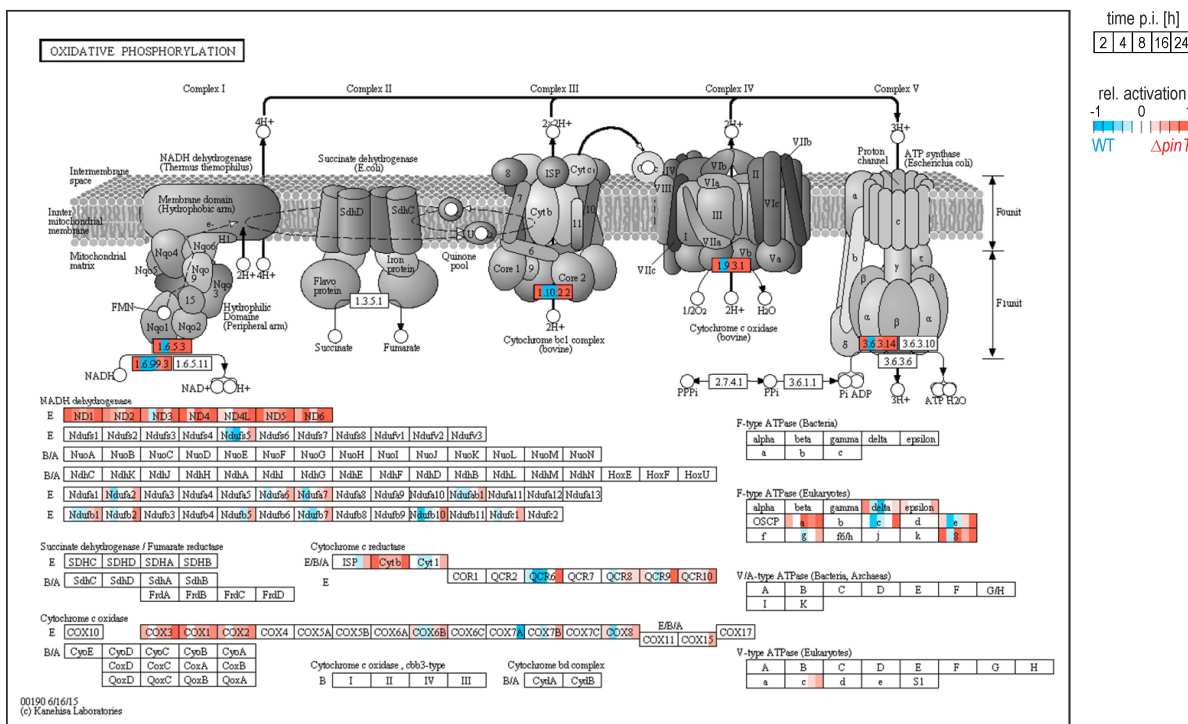
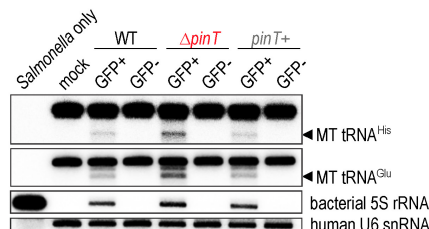
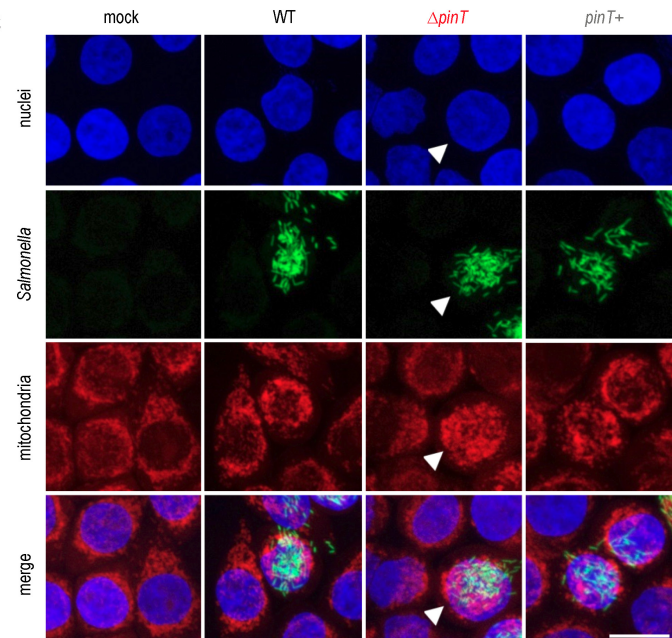
Extended Data Figure 6 | PinT directly targets *Salmonella* *sopE/E2*, *grxA* and *crp* mRNAs. **a**, Volcano plot showing *Salmonella* mRNA levels at 5 min after the pulse-expression of PinT under SPI-1-inducing conditions (LB medium, OD₆₀₀ of 2.0). The data are derived from two biological replicates. Candidates that were confirmed to be directly targeted by PinT are coloured. Red: targets regulated predominantly under SPI-1 conditions; blue: targets regulated (also) under SPI-2 conditions (see panel e). For the full list of changes in gene expression after the PinT pulse see Supplementary Table 1. **b**, RNA duplex formation between PinT and the *sopE* and *sopE2* leaders as predicted by the RNA-hybrid program⁸⁴. Point mutations introduced for compensatory base-pair exchange experiments are indicated. The ribosome binding site and start codon are marked in blue or red, respectively. **c**, Validation of the base-pair interactions as shown in panel b using translational *sopE::gfp* and *sopE2::gfp* reporter gene fusions by compensatory base-pair exchanges. *Salmonella* strains containing both a *gfp* reporter plasmid and an sRNA overexpression vector were grown overnight in LB and analysed by flow cytometry. The error bars indicate s.d. from the mean from biological triplicates. **d**, *In vivo* pulse-expression establishment. GFP-expressing

Salmonella strains harbouring PinT sRNA under an L-arabinose-inducible promoter on a plasmid or corresponding control strains, respectively, were used to infect HeLa-S3 cells. At 4 h p.i., L-arabinose was added to the cell medium. Samples were taken over a time-course of 20 min after the pulse and enriched for *Salmonella* transcripts (see Methods section). PinT sRNA levels were measured by qRT-PCR in the resulting RNA samples and are plotted (mean ± s.d. from technical triplicates). **e**, Pulse-expression of PinT under *in vivo*(-like) conditions (the full data are in Supplementary Table 1). PinT was transiently overexpressed under SPI-2-inducing conditions *in vitro* or 4 h after HeLa-S3 infection (see panel d). In either case, 5 min after induction total RNA samples were taken and analysed by RNA-seq (each two biological replicates). Axes represent fold changes in mRNA abundance between strains harbouring the empty and the PinT-containing plasmid. The two targets validated in panel f are labelled in blue. The *celB* (cellobiose-specific permease IIC component) and *ecnB* (entericidin B precursor) mRNAs might be further targets of PinT (see also panel a), but were not followed up here. **f**, Validation of direct targeting of *grxA* and *crp* mRNAs by the seed region of PinT using translational *grxA::gfp* and *crp::gfp* reporter gene fusions as described for panel c.



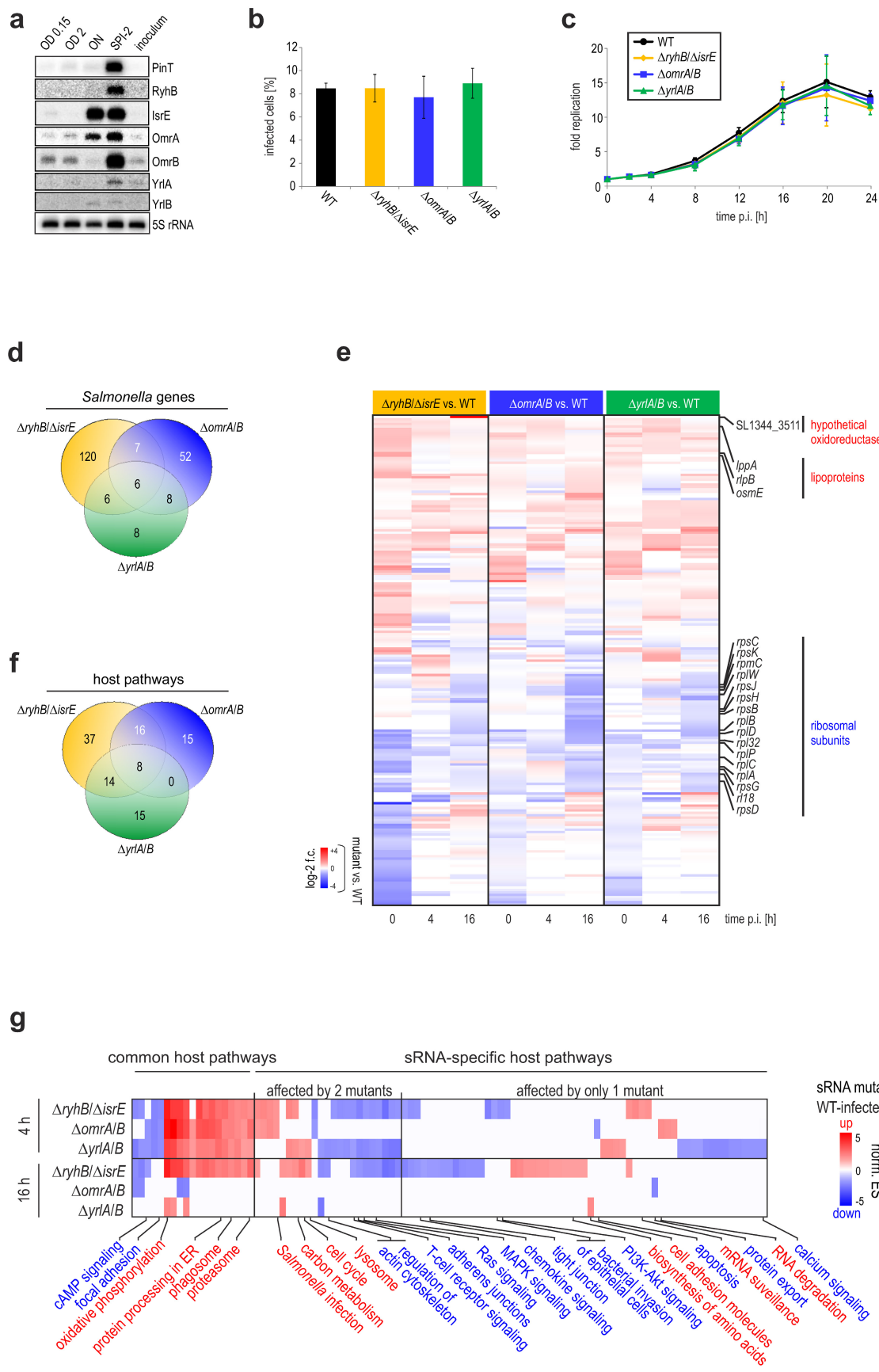
Extended Data Figure 7 | Host expression data for the comparative infection with wild-type or ΔpinT *Salmonella*. **a**, Heat maps showing differentially expressed mRNAs (upper panels), lncRNAs (middle) or miRNAs (lower) between the infection of HeLa-S3 cells with either one of the two indicated *Salmonella* strains and mock-infected controls. Plotted are all genes that were significantly differentially expressed (adjusted P value < 0.05 ; 3 biological replicates) between the indicated conditions for at least one time point during infection. Numbers to the right refer to detected transcripts and transcripts differentially expressed after wild-type infection vs mock, or after ΔpinT infection vs mock, respectively. **b**, PinT affects the expression of coding and noncoding transcripts of the human host. Venn diagrams indicate HeLa-S3 transcripts commonly or specifically regulated compared to mock for the respective infection strain. **c**, Infection with ΔpinT *Salmonella* leads to increased *SOCS3* expression in porcine macrophages. qRT-PCR data (mean \pm s.d.) from biological triplicate experiments of the infection of 3D4/31 cells with *Salmonella* wild-type, ΔpinT , or pinT^+ . Total RNA samples were taken at 6 h p.i. Porcine *GAPDH* mRNA was used for normalization. **d**, qRT-PCR measurement of human *IL8* mRNA in total RNA samples isolated from HeLa-S3 cells at 16 h after either wild-type, ΔpinT or pinT^+ infection

and each sorted into the fractions of invaded (GFP^+) and non-invaded (GFP^-) cells. U6 snRNA was used for normalization. The data represent the mean \pm s.d. from 3 biological replicates. Note that differential gene expression was not caused by different bacterial loads as judged from the ratio of *gfp* mRNA to U6 snRNA ('bacterial load control'). **e**, Enzyme-linked immunosorbent assay for human IL-8 protein in supernatant samples from HeLa-S3 cells at 20 h after their infection with the indicated *Salmonella* strains. Data refer to the mean \pm s.d. from biological triplicate measurements. **f**, Karyogram plot displaying the individual human (female) chromosomes and the genomic position of differentially expressed lncRNA candidates. lncRNAs differentially regulated (adjusted P value < 0.05 ; 3 biological replicates) in response to wild-type infection compared to mock-treated HeLa-S3 cells are indicated as grey bars and candidates differentially expressed between wild-type- and ΔpinT -infected cells as red bars. The position of the bars relative to the respective chromosome indicates the direction of regulation (above the chromosome: upregulation; below: downregulation at the earliest time point when regulation was observed). Panels **c–e**, asterisks denote significantly different transcript (**c, d**) or protein (**e**) levels between wild-type- and ΔpinT -infected cells ($P < 0.05$; one-tailed Mann-Whitney *U*-test).

a**b****c**

Extended Data Figure 8 | Impact of PinT on host mitochondria. **a**, KEGG Pathview representation of oxidative phosphorylation in mitochondria. Dual RNA-seq data of infected HeLa-S3 cells (3 biological replicates) were plotted on top of the pathway map. Individual boxes represent the different time points sampled. Coloured boxes: at the respective time point the given gene(-cluster) was hyper-activated (red) or suppressed (blue) in ΔpinT -infected compared to wild-type-infected cells. **b**, Northern blot detection of mitochondrial tRNAs (shown in Fig. 4e) in HeLa-S3 cells infected for 16 h with the indicated *Salmonella* strains and sorted for GFP⁺ and GFP⁻

fractions. *Salmonella* 5S rRNA serves as a bacterial and human U6 snRNA as a host control. The ‘*Salmonella* only’ sample demonstrates specificity of the probes against the respective human (but not bacterial) tRNAs. For gel source data, see Supplementary Fig. 1. **c**, Elevated mitochondrial expression in response to ΔpinT infection is accompanied by the sub-cellular re-localization of mitochondria in invaded hosts. Mitochondria of infected HeLa-S3 cells were stained using the MitoTracker Orange dye (Life Technologies) and nuclei with Hoechst (Invitrogen). The scale bar indicates 15 μm . The white arrowhead marks a prominent cluster of re-localized mitochondria.



Extended Data Figure 9 | See next page for caption.

Extended Data Figure 9 | Comparative dual RNA-seq experiments with further sRNA mutant *Salmonella*. **a**, Northern blot detection of additional sRNAs induced upon host cell invasion (see Fig. 2a). ‘Inoculum’ refers to bacteria in DMEM. Gel source data in Supplementary Fig. 1. **b**, HeLa-S3 invasion efficiency of the three indicated sRNA double mutants and wild-type *Salmonella* (m.o.i. of 5). **c**, Intracellular replication kinetics of the same strains inside HeLa-S3 (m.o.i. of 5). Data in panels **b** and **c** are derived from flow cytometry measurements as described for Extended Data Fig. 1a, b, and refer to the mean \pm s.d. from 3 biological replicates. **d**, Dual RNA-seq data of the infection of HeLa-S3 cells with the indicated *Salmonella* strains at 0 h, 4 h, and 16 h p.i. The Venn diagram shows the number of significantly (adjusted *P* value < 0.05) differentially expressed *Salmonella* genes (combined for all three time points) between wild-type *Salmonella* and the respective sRNA double mutant strain. **e**, Heat map of bacterial mRNA and sRNA expression changes for $\Delta omrA/B$, $\Delta ryhB/\Delta isrE$ and $\Delta yrlA/B$ as compared to wild-type

Salmonella at 0 h, 4 h and 16 h p.i. of HeLa-S3 cells. Plotted are all genes (except the respectively deleted sRNAs) that were significantly differentially expressed (adjusted *P* value < 0.05) for at least one of the indicated conditions. The gene for a putative oxidoreductase (*SL1344_3511*) was specifically upregulated in intracellular $\Delta ryhB/\Delta isrE$ mutants compared to wild-type *Salmonella*. Many genes for ribosomal subunits were downregulated in all three mutant strains compared to the wild-type. **f**, Venn diagram for the number of commonly or specifically affected human pathways between *Salmonella* wild-type infection and that of the three mutant strains (further specified in panel **g**). **g**, Infection of HeLa-S3 with three sRNA double mutant strains affects distinct sets of host pathways as compared to wild-type infection. Shown are normalized enrichment scores (norm. ES) from a human gene set enrichment analysis (adjusted *P* value < 0.05). The dual RNA-seq data in panels **d–g** were derived from 3 biological replicate experiments.